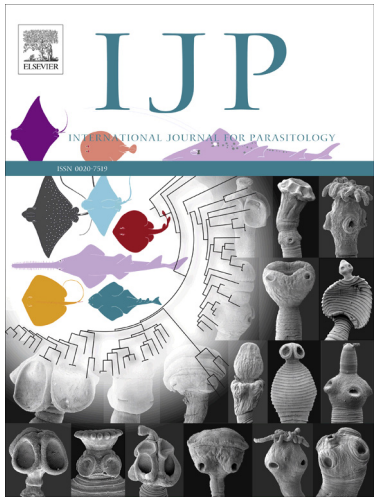

Plasmodium falciparum export protein PFE60 influences Maurer's cleft architecture and virulence complex composition

Meng Zhang, Pierre Faou, Alexander G. Maier, Melanie Rug

PII: S0020-7519(17)30302-8
DOI: https://doi.org/10.1016/j.ijpara.2017.09.003
Reference: PARA 4006

To appear in: *International Journal for Parasitology*

Received Date: 11 May 2017
Revised Date: 20 August 2017
Accepted Date: 6 September 2017

Please cite this article as: Zhang, M., Faou, P., Maier, A.G., Rug, M., *Plasmodium falciparum* export protein PFE60 influences Maurer's cleft architecture and virulence complex composition, *International Journal for Parasitology* (2017), doi: https://doi.org/10.1016/j.ijpara.2017.09.003

Plasmodium falciparum export protein PFE60 influences Maurer's cleft architecture and virulence complex composition

Meng Zhang [a], Pierre Faou [b], Alexander G. Maier [a,1], Melanie Rug [c,1,*]

[a] *Research School of Biology, The Australian National University, Canberra, ACT 2601, Australia*

[b] *Department of Biochemistry and Genetics, La Trobe Institute for Molecular Science, La Trobe University, Melbourne, Victoria 3086, Australia*

[c] *Centre for Advanced Microscopy, The Australian National University, Canberra, ACT 2601, Australia*

[1] These authors contributed equally to the work.

[*]Corresponding author. Melanie Rug, Centre for Advanced Microscopy, The Australian National University, Garran Road #131, ACT Acton 2601, Australia. Tel.: +61 61257649.

E-mail address: melanie.rug@anu.edu.au

Note: Supplementary data associated with this article can be found in the online version, at doi….

Abstract

Plasmodium falciparum, the most lethal malaria parasite species for humans, vastly remodels the mature erythrocyte host cell upon invasion for its own survival. Maurer's clefts (MCs) are membraneous structures established by the parasite in the cytoplasm of infected cells. These organelles are deemed essential for trafficking of virulence complex proteins. The display of the major virulence protein, *P. falciparum* erythrocyte membrane protein 1 (PfEMP1) on the surface of the infected red blood cell (RBC) and the subsequent cytoadhesion of infected cells in the microvasculature of vital organs is the key mechanism that leads to the pathology associated with malaria infection. In a previous study we established that PFE60 (PIESP2) is one of the protein components of this complex. Here we demonstrate that PFE60 plays a role in MC lamella segmentation since in the absence of the protein, infected cells display a higher number of stacked MCs compared with wild type (WT) infected RBCs. Also, another exported parasite protein (Pf332) failed to localise correctly to the MCs in cells lacking PFE60. Furthermore - unlike all other described resident MC membrane proteins - PFE60 does not require its transmembrane regions to be targeted to the organelle. We also provide further evidence that PFE60 is not a RBC surface antigen.

Keywords: Malaria, *Plasmodium falciparum*, Protein trafficking, Maurer's clefts, PFE60, PF3D7_0501200, PIESP2

1. Introduction

The most lethal malaria parasite for humans, *Plasmodium falciparum*, establishes an elaborate trafficking machinery in its newly invaded host cell, the mature human red blood cell (RBC) (Maier et al., 2009; Rug et al., 2014). In order to establish survival mechanisms (e.g. immune evasion, uptake of nutrients, disposal of waste products), the parasite relies on transport of numerous proteins across its own confines, the parasite plasma membrane (PPM), its surrounding parasitophorous vacuole (PV) and its membrane (PVM), and across the RBC cytoplasm to reach their final destinations. Destinations include newly established membraneous structures in the RBC such as Maurer's clefts (MCs) and the RBC membrane (RBCM). Over 300 proteins have been predicted to be transported across the PV into the RBC via a PEXEL (*Plasmodium* export element)/HT (host targeting) signal (Hiller et al., 2004; Marti et al., 2004; Sargeant et al., 2006; Singh et al., 2007) and an unknown number are exported via different signals (PEXEL/HT negative export proteins (PNEPs); (Blisnick et al., 2000; Spycher et al., 2003; Hawthorne et al., 2004; Spielmann et al., 2006; Heiber et al., 2013)). About 60 of the identified genes of the exportome encode the variant expression of *P. falciparum* Erythrocyte Membrane Protein 1 (PfEMP1) (Dzikowski et al., 2006; Voss et al., 2006). This protein is the major virulence factor on the surface of *P. falciparum*-infected erythrocytes and is anchored in parasite-induced protrusions of the RBC membrane, so-called knobs, elevating the protein above other surface proteins. PfEMP1 is part of an elaborate protein complex (virulence complex) including knob- and RBC membrane-associated proteins as well as MC-associated proteins (e.g. PfEMP1 transport protein (PTP1), *P. falciparum* Erythrocyte Membrane Protein 3 (PfEMP3), knob-associated histidine rich protein (KAHRP) (Waterkeyn et al., 2000; Wickham et al., 2001; Maier et al., 2009; Rug et al., 2014). The virulence complex confers adhesion of infected RBCs (iRBCs) to endothelial receptors on the microvasculature of vital organs (Baruch et al., 1995; Su et al., 1995; Smith et al., 2000). Parasites use this survival strategy to avoid being circulated through the spleen and detected by the immune system

(Buffet et al., 2011). For the patient, however, the sequestration and consequent blockage of blood vessels has devastating outcomes, in many cases leading to coma and death (Beeson and Brown, 2002).

Correct trafficking of virulence complex components including PfEMP1 depends on proper assembly and function of MCs (Kilian et al., 2013; Rug et al., 2014). These organelles are established by the parasite in the early intraerythrocytic stages (Grüring et al., 2011) and display an electron dense membrane lining and a translucent lumen in ultrastructural studies. Many resident and transiently associated MC proteins have been described in earlier studies (for review see Mundwiler-Pachlatko and Beck (2013)) but the organelle's biogenesis and exact function in establishing the virulence complex are still enigmatic.

In a previous targeted mutagenesis screen we identified several proteins essential for proper PfEMP1 transport and display (Maier et al., 2008). One of these proteins, PTP1, is crucial for trafficking PfEMP1 to the surface of the iRBC (Rug et al., 2014). In its absence, MCs are reduced to rudimentary globules which are not anchored to the knob structures by actin unlike in wild type (WT) iRBCs. One of the interacting proteins of PTP1 was found to be PFE60, a protein of so far unknown function.

In this work we characterized the PEXEL-containing protein PFE60 (F3D7_0501200.1) in order to further evaluate its function in the asexual life cycle of the malaria parasite and the protein's MC targeting.

2. Materials and methods

2.1. Plasmodium falciparum culture maintenance, synchronization and enrichment

CS2 strain parasites (Salanti et al., 2004) were maintained in in vitro culture according to standard protocols (Maier and Rug, 2013). To maintain knob-positive iRBCs, the cultures were routinely enriched by gelatin flotation (Waterkeyn et al., 2001). Tight synchronization of

the cultures was achieved using sorbitol (Lambros and Vanderberg, 1979).

2.2. Construct design, transfection and Southern blot analysis of transgenic cell lines

To generate the CS2/PFE60-hemagglutinin/strep-tag (CS2/PFE60-HA/strep) cell line, *PFE60* was cloned into the pHAST-1 vector (Rug and Maier, 2013) using oligonucleotides aw801 and aw802 (for oligonucleotide sequences see Supplementary Table S1). For the PFE60-GFP cell line, the 3' of the full-length *PFE60* gene was cloned into the pGREP-1 vector (Rug and Maier, 2013) (using oligonucleotides: al238 and al239; Supplementary Fig. S1). For the PFE60ΔTM-GFP cell line, the 3' *PFE60* coding region lacking the C-terminal transmembrane (TM) domains was cloned into the pGREP-1 vector (oligonucleotides: al238 and al243). The constructs were transfected into CS2 WT parasites and positively selected by adding WR99210 (Jacobus Pharmaceutical Company Inc., US) as previously described (Rug and Maier, 2013). The ΔPFE60 cell line was generated previously (Maier et al., 2008).

The parasite genomic DNA was extracted using the DNeasy blood and tissue kit (Qiagen, Australia) and integration of the plasmids into the parasite genome was confirmed by Southern blot analysis using the digoxigenin (DIG) system according to standard protocols (Roche, Germany).

To generate the complementation cell line, ΔPFE60/PFE60-GFP(comp), the putative endogenous promoter of *PFE60* (1 kb upstream of *PFE60* coding sequence) (oligonucleotides: al359 and al365) and *PFE60* sequence (oligonucleotides: al366 and al367) were cloned into the pGLUX-6 vector by Gibson cloning (NEB, Australia) and transfected into ΔPFE60 iRBCs with subsequent positive selection by adding puromycin (100 ng/ml; Invivogen, Hong Kong) (Tran et al., 2014). All plasmids were sequenced before transfection (Micromon, Melbourne, Australia).

2.3. Surface exposure of PFE60

2.3.1. Live cell imaging and immunofluorescence microscopy

Immunofluorescence microscopy was performed on acetone/methanol (90%/10%) fixed smears as previously described (Rug et al., 2014). Cells were probed with primary antibodies: rabbit anti-GFP (1:1000), mouse anti-HA (1:100, Roche, clone 3F10), rabbit anti-PFE60 (1:1000, (Maier et al., 2008)), mouse anti-ATS (1:50, (Knuepfer et al., 2005)), rabbit anti-skeleton-binding protein 1 (SBP1) (1:500, (Rug et al., 2014)), mouse anti-PfEMP3 (1:1000; (Waterkeyn et al., 2000)), mouse anti-PTP1 (1:500; (Rug et al., 2014)), rabbit anti-*Plasmodium* Transport Protein 2 (PTP2) (1:500, (Regev-Rudzki et al., 2013)), rabbit anti-*P. falciparum* Heat Shock Protein 70x (PfHSP70x) (1:500; (Külzer et al., 2012)), rabbit anti-ring stage protein 1 (REX1) (1:2000) (Hawthorne et al., 2008), mouse anti-Pf332 (1:200; (Hodder et al., 2009)) or rabbit anti-membrane-associated histidine-rich protein 1 (MAHRP1) (1:500; (Spycher et al., 2003)) and subsequently incubated with secondary antibodies Alexa Fluor 594 or 488 conjugated anti-mouse or anti-rabbit IgG (1:500; Thermo Fisher Scientific, Australia). Specimens were mounted with Vectashield containing 2 mg/ml of DAPI (Vector Laboratories, Australia). Both live and fixed specimens were viewed at ambient temperature on a Deltavision Elite microscope using 100x oil objective, NA1.4 (GE Healthcare, Australia) and images captured by a CoolSnap HQ2 or an EMCCD Cascade II/512 high-sensitivity camera and softWoRx software (GE Healthcare). The images were analyzed and edited using ImageJ and Photoshop (Adobe). Adjustments to highlight features of interest were performed equally on controls and cells of interest.

2.3.2. Flow cytometry analysis

iRBCs were enriched by magnet purification. Both live and permeabilized cells were blocked using 0.5% BSA in PBS for 30 min at room temperature. Cells were probed with primary antibodies (rabbit anti-PFE60 (1:250), mouse anti-glycophorin C (1:100, Sigma, Australia)) and subsequently with secondary antibodies (Alexa Fluor 647 conjugated anti-

mouse or anti-rabbit IgG (1:300, Thermofisher)). For intracellular labeling, packed cells were first fixed in 4% paraformaldehyde/0.0075% glutaraldehyde and subsequently permeabilized using 0.1% Triton X-100 in PBS. Flow cytometry was performed using a BD LSRII flow cytometer and BD FACSDiva Software (Becton Dickinson, Australia). Data collected included side scatter, forward scatter and Alexa 647 channel for 100,000 cells/treatment, analysed using FlowJo software (FlowJo, LLC) and processed using Adobe Illustrator.

2.4. Electron microscopy

For scanning electron microscopy, magnet-purified mature stage iRBCs were fixed in 2% glutaraldehyde/PBS (Electron Microscopy Science, EMS, US) and settled on Poly-L-lysine coated coverslips (50 µg/ml (Sigma)), subjected to an ethanol dehydration series and critical point drying (CPD030 (Balzers, Liechtenstein)). Cells were subsequently coated with platinum in a K550X sputter coater (Quorum Technologies, US) at 25 mA and viewed in an UltraPlus FESEM (Zeiss, Germany) at 3 kV accelerating voltage.

For transmission electron microscopy (TEM), magnet-purified mature stage iRBCs were fixed in 4% paraformaldehyde, 2% glutaraldehyde/PBS (EMS), 0.5% OsO_4 (EMS). Cells were en bloc stained with 2% uranyl acetate (EMS) in 1.2% DNA grade low melting agarose (Sigma), subjected to an ethanol dehydration series and subsequently embedded in LR white resin (ProSciTech, PST, Australia). Ultrathin sections (70 nm, EM UC7 ultramicrotome (Leica, Austria)) were retrieved onto 100 mesh carbon coated copper grids with 0.6% formvar film (PST) and contrast stained with 2% aqueous uranyl acetate and Reynold's Lead Citrate (PST) (Rug et al., 2004). Sections were viewed in a H7100FA (Hitachi, Japan) transmission electron microscope at 75 kV accelerating voltage. Images were captured with an Ultrascan and Orius camera and analysed with Gatan Digital micrograph software.

2.5. Quantification of TEM results

The parasite images were coded with numbers and the samples measured were chosen by a random number generator. To increase the analytical rigor each TEM sample preparation was conducted three times. Data are presented as group mean ± S.E.M.. To determine the differences between the lengths of MCs in WT cells, ΔPFE60 and ΔPFE60/PFE60-GFP(comp) cell lines, ANOVA and Tukey-Kramer Multiple Comparisons Test were performed using Prism (Graphpad) and Instats (Graphpad). Data were graphed using Instats and Adobe illustrator CS6.

2.6. Fractionation of iRBCs and analysis by SDS PAGE and western blots

2.6.1. Subcellular fractionation and solubility studies

Saponin lysis was conducted according to Benting et al. (1994). For solubility studies, magnet-purified cells of different asexual life cycle stages were washed in PBS before being lysed in ice-cold water containing Complete™ protease inhibitor (Roche). The pellets were resuspended in 100 mM Na_2CO_3 pH 11.5 and incubated on ice or in 6 M urea in 10 mM Tris-HCl pH 8 containing Complete™ protease inhibitor (Roche) for 1 h (Fujiki et al., 1982; Vincensini et al., 2008). Equal cell quantities of supernatant and washed pellet were taken up in reducing lithium dodecyl sulfate (LDS) sample buffer (Thermo Fisher Scientific) and subjected to SDS PAGE for analysis. Solubility assays on trophozoite-stage iRBCs with Triton X-114 were conducted according to, and modified from, Arnold and Linke (2008). In brief, 4.2 x 10^7 iRBCs were resuspended in 100 µl of PBS containing Complete™ protease inhibitor (Roche). The cell suspensions were solubilized in 100 µl of Triton X-114 buffer on ice. The sample was incubated for 10 min at 37° C and pelleted at 300 *g* for 3 min. Additional Triton X-114 buffer was added to the aqueous phase to a final concentration of 0.5% (w/v) and mixed on ice. After pelleting, the aqueous phase was separated and the two detergent phases were combined (Bordier, 1981). Triton X-114 was removed and the protein was concentrated by using Trichloric acid and acetone in 25 µl of water containing protease inhibitor.

206

207 *2.6.2. Time course western blot*

208 Pellets from tightly synchronized cells were collected at 6 h intervals (6 x 10^5 cells at
209 each time point). Before samples were loaded onto SDS gels, whole cells or saponin-lysed
210 samples were treated with Benzonase (Novagen, US) with Complete™ protease inhibitor and
211 pellets taken up in reducing LDS sample buffer. Proteins were separated in NuPAGE 4-12%
212 Bis tris gels and MOPS (3-(N-morpholino)propanesulfonic acid) SDS running buffer (Thermo
213 Fisher Scientific). Proteins were transferred onto nitrocellulose membranes (iblot, Thermo
214 Fisher Scientific) and probed with primary antibodies: rabbit anti-PFE60 (1:500, (Maier et al.,
215 2008)), mouse anti-HA (1:1000, Roche, clone 3F10), mouse anti-GFP (1:1000, Roche), rabbit
216 anti-EXP1 (1:1000, (Günther et al., 1991)), anti-PFD1170c (1:1000, (Oberli et al., 2014)),
217 mouse anti-PfHSP70 (1:1000, (Pesce et al., 2008)). Secondary antibodies used were goat anti-
218 mouse IgG (H+L)-HRP1 human adsorbed (1:2000, Southern Biotech, US), ECL ™ anti-rabbit
219 IgG Horseradish Peroxidase linked whole antibody from donkey (1:5000, GE Healthcare).
220 Protein bands were visualized using Lumi-light western blotting substrate ECL (Roche). To
221 reprobe, the membrane was incubated in preheated stripping buffer (62.5 mM Tris, pH 6.7,
222 and 20 g/L of SDS) at 70° C twice for 10 min. The membrane was then washed with PBS
223 0.05% Tween-20 for 6 × 10 min before blocking for detection with different antibodies.

224

225 *2.6.3. Trypsin cleavage assay*

226 Magnet-purified trophozoite-iRBCs (10^7; 20-28 h post invasion) or uninfected RBCs
227 were incubated with N-tosyl-L-phenylalanine chloromethyl ketone TPCK-treated trypsin
228 (Sigma, 1 mg/ml in PBS), PBS only or trypsin plus phenylmethane sulfonyl fluoride (PMSF) (5
229 mM) (Sigma) at 37° C for 1 h. The reaction was terminated by the addition of PMSF (5 mM) to
230 all samples. A proportion of the cells from each sample was subjected to live cell imaging. The
231 remaining samples were processed and analyzed as previously described (Waterkeyn et al.,

2000). Western blots containing Triton X-100 soluble fractions were probed with rabbit anti-FFE60 antibodies and mouse anti-GFP antibodies. Blots containing Triton X-100 insoluble/SDS soluble fractions of the sample were probed with mouse anti-ATS antibodies (1:1000).

2.6.4. Pull down assay and MS analysis

Magnet-purified trophozoite-iRBCs (7 x 10^8) were resuspended in 10-15 pellet volumes of ice-cold solublisation buffer TNET (1% Triton X-100, 150 mM NaCl, 100 mM EDTA and 50 mM Tris pH 7.4) containing 1 x Complete™ protease inhibitor and 1 mM PMSF. Samples were gently sonicated with a probe sonicator (Branson Sonifier 250, Thermo Fisher Scientific, Australia) and solubilized at 4° C for 2 h. Samples were pelleted at 16,000 *g* at 4° C for 15 min, supernatant transferred to new tubes and incubated with 100 µl of anti-HA affinity matrix (Roche) at 4° C for 8 h. After pelleting (2,400 *g* for 30 s), the beads were washed three times in PBS containing protease inhibitors. Half of the beads were resuspended in an equal volume of reducing 4x LDS sample buffer, incubated at 70° C for 3 min and analysed by western blot. Proteins from the remaining beads were eluted by incubation in 8 M urea followed by reduction, alkylation and digestion with trypsin as previously described (Caruana et al., 2016). Tryptic peptides were analysed by MS analysis (LTQ Orbitrap Elite ETD Mass spectrometer, Thermo Scientific).

MS/MS spectra were queried using MaxQuant (Cox and Mann, 2008) (version 1.5.5.1) and PlasmoDB (version 13.0). The false discovery rate (FDR) was set to 1% for peptide and protein identifications. Result files were imported to Scaffold Q+S (version 4.7.3, Proteome Software Inc.) for visualisation and validation. Peptide identifications were accepted if those could be established at greater than 10.0% probability to achieve an FDR less than 1.0% by the Peptide Prophet algorithm (Keller et al., 2002) with Scaffold delta-mass correction. Protein identifications were accepted if those could be established at greater than 94.0% probability to achieve an FDR

less than 1.0% and contained at least two identified peptides. Protein probabilities were assigned by the Protein Prophet algorithm (Nesvizhskii et al., 2003). Proteins that contained similar peptides and could not be differentiated based on MS/MS analysis alone were grouped to satisfy the principles of parsimony. Putative interaction proteins were considered significant if those showed at least two identified peptides and were detected in each repeat of the above experiment (two independent pull down assays). Quantitative values were calculated using the TOP 3 method (Silva et al., 2006) using the quantification analysis method "Top 3 Precursor Intensity" and normalisation from Scaffold.

2.6.5. Data and materials availability

The MS proteomics data have been deposited to the ProteomeXchange Consortium via the PRIDE partner repository with the dataset identifier PXD006826 and 10.6019/PXD006826.

3. Results

3.1. The MC protein PFE60 is not exposed on the surface of the RBC

PFE60 has been described as a surface protein in early reports (Florens et al., 2004) resulting in the name, *Plasmodium* infected erythrocyte surface antigen/protein (PIESA2 or PIESP2). Subsequently, Vincensini et al. (2005) used isotope metabolic labeling of ghost fractions and reported the protein to be localized on MCs on intact and permeabilised ghosts, naming it PFE60 according to its previous annotation in PlasmoDB (**PFE0060w**, now **PF3D7_0501200**).

In order to resolve these previously reported discrepancies on the localization of PFE60, we performed flow cytometry analysis. Here, we subjected live PFE60-GFP iRBCs to treatment with anti-PFE60 antibodies and compared them with unlabeled live cells. The flow cytometry histogram in Fig. 1Aa clearly demonstrates that both curves overlap entirely,

suggesting absence of PFE60 antigen on the surface of these cells. In order to demonstrate the reactivity of the secondary antibody we subjected the cells to permeabilisation before labeling and found a strong signal deriving from the intracellular pool of PFE60 protein (Fig. 1Ab). Furthermore, we demonstrated that a known RBC surface marker, Glycophorin A, could be readily detected on the surface of live cells, confirming the validity of the live cell flow cytometry assay (Fig. 1Ac). To provide additional evidence of the absence of PFE60 on the surface of iRBCs we conducted systematic immunofluorescence assays using markers for various compartments in the iRBCs, which have been implicated in playing crucial roles in the transport of virulence complex or surface proteins (Fig. 1). In our co-localisation studies on fixed cells we used marker proteins for the iRBC membrane and MCs, J-Dots and Electron Dense Vesicles (EDVs), transport vesicles thought to be crucial in assembly of the virulence complex (Waterkeyn et al., 2000; Külzer et al., 2010; Regev-Rudzki et al., 2013; Rug et al., 2014).

We could not observe co-localisation of PFE60 with PfEMP3, an exported protein associated with the host cell membrane skeleton (Pasloske et al., 1993; Waller et al., 2007) at any stage of the asexual life cycle (Fig 1B). Furthermore, PFE60 did not co-localise with PTP2, a marker of EDVs (Fig. 1B), and there was very little co-localisation with HSP70x, a marker of J-dots, small transport vesicles involved in PfEMP1 trafficking (Fig. 1B) (Külzer et al., 2010). However, a strong overlap in fluorescence signal could be observed with two MC resident proteins, SBP1and PTP1 (Blisnick et al., 2000; Rug et al., 2014) in all stages throughout the asexual life cycle (Fig. 1B).

Additionally, we generated a cell line where the full-length PFE60 protein was C-terminally tagged with GFP (PFE60-GFP) by replacing the endogenous gene with a gene encoding for the tagged chimera (Supplementary Fig. S1A). We subsequently performed trypsin cleavage assays on magnet-purified PFE60-GFP iRBCs. Exposure of PFE60 on the surface of iRBCs can be detected by exposing intact iRBCs to trypsin treatment - surface

exposed proteins would be cleaved. Live fluorescence microscopy (Fig. 1C) clearly demonstrates that the GFP signal can still be detected after treating intact PFE60-GFP iRBCs with trypsin (Fig. 1C) similar to untreated controls and controls including a trypsin inhibitor (PMSF) (Fig. 1C). We confirmed these findings by western blot analysis, firstly probed with anti-GFP antibody detecting the C-terminal part of the protein chimera and subsequently probed with anti-PFE60 antibody detecting the N-terminal part (Fig. 1D). If either of the termini were exposed on the surface of the iRBC, we would expect a cleaved product upon exposure to trypsin. Fig. 1C demonstrates that both antibodies detected the full-length PFE60 protein in the presence and absence of trypsin, indicating that PFE60 is not located on the surface of the host erythrocyte but rather protected within the iRBC (Fig. 1D). The Triton X-100 insoluble/SDS soluble fraction was probed with a control antibody against PfEMP1, a surface exposed protein that is readily cleaved by trypsin. The conserved C-terminal part (ATS) of PfEMP1, which is protected within the cell, was detected as a smaller size fragment on the blot after cleavage with trypsin (Fig. 1D). These studies provide further evidence that PFE60 is a MC resident protein that is not exposed on the iRBC surface.

3.2. The putative TM domains anchor PFE60 in the MC membrane

In an effort to address the function of the putative TM domains of PFE60, we generated a GFP-cell line where the two putative TM domains of the protein were deleted (PFE60ΔTM-GFP), in addition to the above-described full-length PFE60-GFP cell line (Fig. 2A). Both constructs were integrated into the parasite genome and the proteins were expressed from the endogenous locus (Supplementary Fig. S1A, B). In live cells the GFP signal in the PFE60-GFP cell line was observed in punctate structures in the host erythrocyte (Fig. 2B) throughout the asexual life cycle, a pattern reminiscent of MCs. This was confirmed in immunofluorescence assays on fixed cells where the GFP signal co-localised with the MC marker PTP1 (Fig. 2C). Surprisingly, PFE60ΔTM-GFP also displayed a punctate pattern in live

cells (Fig. 2B) and co-localised with PTP1 (Fig. 2C). To our knowledge this is the first report of a MC protein still targeted to MCs in the absence of its TM domain.

We next investigated the membrane binding capabilities of the two proteins in biochemical solubility assays (Fig. 2D). Both proteins were found in the detergent fraction on western blots probed with anti-GFP antibodies when subjected to Triton X-114 (Fig. 2D), indicating a membrane association of both proteins. To determine the nature of membrane interaction, we further subjected both cell lines to urea and carbonate extractions. Upon urea treatment, a much larger proportion of the PFE60ΔTM-GFP protein could be solubilized compared with the full-length protein, indicating a peripheral membrane association for PFE60ΔTM-GFP (Fig. 2D). Similarly, PFE60ΔTM-GFP was readily soluble in Na_2CO_3, whereas only a minor proportion of PFE60-GFP could be solubilised upon carbonate fractionation in all stages of the erythrocytic life cycle (Fig. 2D, Supplementary Fig. S2A). These results demonstrate that full-length PFE60 is an integral membrane protein with the TM domain responsible for integration into the membrane (Fig. 2D).

3.3. PFE60 knock-out phenotype

In a previous high-throughput gene deletion study of exported proteins, PFE60 was targeted as a potential candidate involved in trafficking of the major virulence factor PfEMP1 (Maier et al., 2008). We determined that in the absence of PFE60 (ΔPFE60), PfEMP1 was still trafficked to the surface of the infected erythrocyte (Maier et al., 2008).

To further assess the functional consequences of a PFE60 gene deletion, we studied trafficking of additional exported proteins known to be involved in establishing the virulence complex. No significant differences could be detected in the trafficking patterns for the markers of J-dots (HSP70x), for PfEMP1 and PfEMP3 in immunofluorescence assays (Supplementary Fig. S2B). Subsequently, we chose five MC proteins to study potential trafficking defects in the absence of PFE60. Four of the known MC resident proteins, PTP1,

SBP1, REX1 and MAHRP1, showed no differences in localization patterns in the absence of PFE60 compared with WT (Fig. 3A).

Interestingly, the pattern for Pf332, another component of the virulence complex, was significantly different in the ΔPFE60 compared with the WT cell line. The punctate pattern in the ΔPFE60 cell line was mainly localized around the parasite membrane and in a few areas in the RBC instead of the typical MC distribution all across the RBC cytoplasm in the WT cell line. Co-labelling with another MC resident protein (REX1) confirmed that Pf332 was not located on MCs (Supplementary Fig. S2C). In order to rule out bias in the analysis of the immunofluorescence assays, we performed quantitative analysis on cells that had been dual-labeled with anti-Pf332 and anti-REX1 in ΔPFE60 versus WT iRBCs. By comparing the average integrated fluorescence density in 28 cells for each labeling in both cell lines, we confirmed that Pf332 is not only mislocalised in ΔPFE60 but the Pf332 fluorescence signal is reduced to almost half in ΔPFE60 versus WT iRBCs (Supplementary Fig. S2D, WT Pf332 versus ΔPFE60 Pf332). Co-labelling with REX1 was used as a control in the same cells and neither protein localization nor average integrated fluorescence density changed significantly in the absence of PFE60 (Supplementary Fig. S2D, WT REX1 versus ΔPFE60 REX1). We also determined the amount of punctae, representing MCs, observed in projections of whole cell immunofluorescence assay analysis. We found that a lower number (P>0.05) was detected in ΔPFE60 versus WT iRBCs (Supplementary Fig. S2E). One reason why the number was not significantly reduced in ΔPFE60 iRBCs could be that the resolution of light microscopy might not consistently differentiate between individual lamellae and stacks of MCs.

In order to identify an influence on the presence of knobs in the absence of PFE60 we performed scanning electron microscopy analysis. Cells showed similar appearance and distribution patterns of knobs on the surface of the infected erythrocyte in the presence and absence of PFE60 (Fig 3B).

To verify the phenotypes we generated a complementation cell line where a full-length PFE60 protein tagged with GFP was episomally expressed under the putative endogenous PFE60 promoter region in the ΔPFE60 cell line (ΔPFE60/PFE60-GFP(comp)) (Supplementary Fig. S1C). In order to confirm correct expression during the asexual life cycle we compared full-length PFE60 expression from the endogenous gene locus (PFE60-GFP) with the episomal expression of PFE60-GFP in the ΔPFE60/PFE60-GFP(comp) cell line. Western blot analysis demonstrated that both proteins are expressed at very similar levels and times in the asexual life cycle (Fig. 4A). Western blot analysis also confirmed proteins of the expected molecular mass (49 kDa and 76 kDa) for the native protein versus the episomally expressed GFP-tagged version, respectively, and the absence of the protein in the ΔPFE60 cell line (Supplementary Fig. S2F).

In order to study potential ultrastructural differences in the WT, ΔPFE60 and ΔPFE60/PFE60-GFP(comp) cell lines, we subjected them to a detailed electron microscopical analysis. TEM revealed significant morphological differences in the MC architecture in the ΔPFE60 cell line compared with the WT and ΔPFE60/PFE60-GFP(comp) cells. The MCs seemed shorter and occured more frequently in stacks in ΔPFE60 versus WT cells (Fig. 4B). To fully verify these differences, a quantitative analysis was performed, where 90 MCs (of 30 randomly chosen MCs in three independent experiments each) were measured and their architecture documented. As shown in Fig. 4C ΔPFE60 iRBCs contain a significantly higher percentage of stacked MCs in comparison to WT iRBCs: almost 20% of the MCs in the knock-out were arranged in stacks, whereas in WT iRBCs only 2% of MCs displayed a stacked phenotype (mean ± S.E.M., 18.9 ± 4.1 versus 2.2 ± 1.6 average percentage of stacked MCs, respectively) confirming our quantitative immunofluorescence results of a lower number of punctae of MCs in ΔPFE60 (Supplementary Fig. S2E). The low level of MC stacks found in WT

411 iRBCs was restored by complementation of PFE60 (mean ± S.E.M., ΔPFE60/PFE60-GFP(comp)
412 iRBCs 5.6 ± 2.4 versus WT 2.2 ± 1.6 average percentage of stacked MCs, respectively).

413 We also examined the length of randomly chosen MCs in three independently
414 performed experiments for each cell line (>30 clefts/cell line/experiment). As shown in Fig.
415 4D, MCs were significantly shorter in ΔPFE60 in comparison to MCs in WT iRBCs (mean ±
416 S.E.M., 282.3 ± 10.9 nm versus 471.1 ± 15.4 nm MC average length, respectively). This
417 phenotype could only be partially restored in ΔPFE60/PFE60-GFP(comp) iRBCs (mean ±
418 S.E.M.; ΔPFE60/PFE60-GFP(comp) 336.7 ± 11.7 nm versus WT 471.1 ± 15.4 nm average MC
419 length, respectively).

420

421 *3.4. Interacting partners*

422 Since MCs are docking and possibly sorting points for virulence complex proteins (e.g.
423 KAHRP, PfEMP1) en route to the RBC membrane and seem to be playing an essential role in
424 the assembly of this complex (Wickham et al., 2001; Rug et al., 2014), we investigated
425 potential interacting partners of PFE60. To explore this, we generated a cell line where the
426 PFE60 protein was C-terminally tagged with a triple hemagglutinin/Strep tag and expressed
427 from the endogenous gene locus (PFE60-HA/strep; Supplementary Fig. S1D). We employed
428 immunoprecipitation assays where cell lysates from the PFE60-HA/Strep cell line were
429 incubated with anti-HA coupled beads. WT cells were used as a control in each experiment. In
430 order to investigate potential interacting partners, we subjected the eluates of the
431 immunoprecipitation assays to MS analysis. We identified potential proteins as binding
432 partners after affinity purification followed by MS from two independent experiments
433 (Supplementary Table S2). Interestingly, SBP1, Pf332 and MAHRP1 were identified as
434 potential binding partners with high fidelity (quantitative value >1.00E+07) in both analyses,
435 all of those being MC resident proteins (Table 1). Furthermore, PFE0050w was pulled down,

436 a protein that has previously been described to be in a similar location as PFE60 (Florens et
437 al., 2004).

438 Protein eluates from the pull down assay were further analysed via western blot
439 analysis to confirm binding partners identified in the MS analysis (Fig. 5). When probed with
440 anti-HA antibody, the pull down eluate of the PFE60-HA/strep cell line displayed a band at the
441 expected molecular mass in contrast to the control WT cell line. Furthermore, the specific
442 band could only be observed in the eluate after binding, not in the flow-through. The blot was
443 then stripped and re-probed with anti-SBP1 antibody. Interestingly, a specific band of the
444 molecular mass corresponding to SBP1 could be detected in the eluate from the PFE60-
445 HA/strep cell line whereas no band of a corresponding size was detected in the control WT
446 cell line, confirming interaction of PFE60 with SBP1. Consistent with this finding, more SBP1
447 protein was found in the flow-through for the WT cell line and less of the protein could be
448 detected in the PFE60-HA cell line unbound fraction (Fig. 5A). In reciprocal experiments, we
449 were able to immunoprecipitate endogenous untagged PFE60 from WT cells with anti-SBP1
450 antibodies and endogenous SBP1 with anti-PFE60 antibodies (Fig. 5B). These results and the
451 fact that PFE60 and SBP1 co-localise at MCs in immunofluorescence assays (Fig. 1A) indicate
452 interaction of PFE60 with SBP1 on MCs.
453
454 **4. Discussion**
455 MCs can be detected as early as ring stages (Langreth et al., 1978; Bannister et al.,
456 2004; Grüring et al., 2011) and they prevail within the RBC even after merozoite release.
457 Many proteins that are transiently or permanently associated with MCs have been described
458 over the years (for review see Mundwiler-Pachlatko and Beck (2013)) but the exact function
459 of these organelles is still enigmatic. Since export of proteins and transport through MCs is
460 key to malaria parasite survival and establishment of disease, it is imperative to identify and
461 characterize more proteins of the "Cleftome" in order to fully understand the role and

462 importance of these organelles in the development of malaria pathogenesis.

463 Here, we report on a protein that was identified in an earlier study as an interacting
464 partner of PTP1, one of the proteins essential for correct trafficking of the major virulence
465 factor PfEMP1 to the surface of the *P. falciparum*-infected RBC (Rug et al., 2014). In the
466 current study, we found striking phenotypical differences when comparing WT with ΔPFE60
467 iRBCs. In the absence of PFE60, the clefts were shorter and occured more frequently in stacks
468 than in WT iRBCs. Expression of the deleted gene from an episomal locus (ΔPFE60/PFE60-
469 GFP(comp)) restored the single lamellae MC phenotype usually observed in CS2 WT cells. The
470 reduced length of the MCs could only be partially complemented, which might indicate that
471 expression from the endogenous gene locus is important for the proper formation of MCs.
472 Furthermore, we found that Pf332, a MC resident protein, was not trafficked to MCs in the
473 absence of PFE60. Interestingly, the phenomenon of stacked MCs has been described earlier
474 in gene deletion cell lines for Pf332 (Glenister et al., 2009) and REX1 (Hanssen et al., 2008;
475 Dixon et al., 2011). In comparison with PFE60, these proteins are significantly larger (689 kDa
476 and 83 kDa, respectively, versus 49 kDa for PFE60) and seem to be only peripherally
477 associated with MC. Their highly negatively charged C-terminal domains were suggested to be
478 involved in segregation of MC lamellae (Hanssen et al., 2008; Glenister et al., 2009; Nilsson et
479 al., 2012). PFE60 is the first integral MC protein involved in MC lamellar segregation.

480 It has been proposed earlier that Pf332 might interact with a membrane bound protein
481 (Nilsson et al., 2012) to exert its full function. In our pull down and MS analysis we found
482 Pf332 as a potential interaction partner of PFE60. It is therefore intriguing to speculate that in
483 the absence of PFE60, Pf332 is not as tightly associated with MCs as in its presence and hence
484 cannot fulfill its function to segregate MC lamellae efficiently. Our immunofluorescence assay
485 confirmed this hypothesis with Pf332 being localized in punctate areas in the RBC cytoplasm
486 but not in MCs. Therefore, the interaction of Pf332 and PFE60 on MCs seems to be crucial for

proper segregation and formation of full-length MCs. It is worth noting that Pf332, PFE60 and REX1 are only found in the Laveranian group of *Plasmodium* spp., indicating their significance in MC assembly and PfEMP1 surface display. Dissecting the roles of other potential interaction partners (Supplementary Table S2) might provide further insights into the functional mechanisms of MCs.

Amongst the known integral MC membrane proteins, two different classes have been described with one containing a PEXEL/HT signal to cross the translocon within the PV (e.g. PTP1 (Maier et al., 2008; Rug et al., 2014); STEVORs (Przyborski et al., 2005); type A RIFINS (Khattab and Klinkert, 2006); Pfmc-2TMs (Sam-Yellowe et al., 2004), Surfin (Winter et al., 2005). The other class of integral MC proteins does not contain a PEXEL (PNEPs) and seems to depend on the TM domain for transport and MC association (e.g. SBP1 (Saridaki et al., 2009) and REX2 (Haase et al., 2009)). All previous reports on MC proteins containing a TM domain indicate that trafficking to MCs involves two steps, translocation across the PV and subsequent targeting to MCs (Sam-Yellowe, 2009; Deponte et al., 2012; Heiber et al., 2013). Here, we describe the first PEXEL-containing integral membrane protein that is targeted to MCs independently of its TM domains. Both PFE60-GFP and PFE60ΔTM-GFP cell lines displayed the GFP-tagged protein on MCs as shown in live cells and in co-localisation experiments with previously described MC marker proteins. Biochemically, a TM protein is usually defined as such if it cannot be extracted from the membraneous fraction by urea or sodium carbonate but only in the presence of a detergent (Schook et al., 1979; Fujiki et al., 1982). The full-length PFE60 protein clearly displays features of an integral membrane protein with the majority of the protein resisting extraction in the chaoptropic agent urea or high pH sodium carbonate, indicating a protein-lipid interaction in the MC membrane similar to that previously described for the two TM MC protein family (PfMC-2TM) (Bachmann et al., 2015) and Exp1 (Günther et al., 1991). These results identify PFE60 as a resident integral MC membrane protein. The truncated form missing the TM domains seems to be more readily

513 extractable in urea or carbonate buffer (Schook et al., 1979; Fujiki et al., 1982), hence
514 PFE60ΔTM-GFP only seems to be peripherally associated with other proteins on MCs, without
515 dissociation of the lipid bilayer. Bioinformatic analysis using GPS-Lipid 1.0 (Xie et al., 2016)
516 revealed the presence of a weak S-palmitoylation motif at amino acid 370 of the protein.
517 However, this motif is deleted in the PFE60ΔTM-GFP cell line and therefore does not provide
518 a satisfactory explanation for the peripheral membrane association of the truncated protein.
519 Taken together these results demonstrate that targeting PFE60 to MCs is not dependent on
520 the two TM domains but the protein cannot be anchored in the membrane without these
521 domains being present.

522 There has been controversy in the literature about the location of PFE60 with one
523 group (Florens et al., 2004) arguing that the protein might be transiently associated with MCs
524 on its way to the surface of the RBC membrane and another group (Vincensini et al., 2005)
525 describing PFE60 as a MC resident protein. Both groups used different methodologies for
526 labeling the protein (biotin versus isotope metabolic labeling, respectively). The latter group
527 offered the possibility that schizonts used in the assay in the Florens et al. (2004) study might
528 be permeable to biotin and therefore MCs might have been labeled and mistaken for surface
529 labeling. Alternatively, PFE60, due to its transient association with MCs on its way to the RBC
530 surface might only be detectable on MCs in IFA due to a higher concentration of the protein in
531 these organelles compared with a spread across the iRBC surface. Our results confirm the
532 observations by Vincensini et al. (2005) that PFE60 indeed is not exposed on the RBC surface.
533 The live cell assay with trypsin digestion of potentially exposed protein domains clearly
534 demonstrates that the GFP fluorescent signal is detected in the presence and absence of
535 trypsin, indicating that the C-terminus is not exposed on the surface of the live cells with
536 western blot analysis confirming that neither the N- nor the C-terminus are externally
537 exposed.

Taken together, we have characterized the function of PFE60 in the asexual stages of *P. falciparum* iRBCs as being important for MC architecture. PFE60 is the first integral MC resident protein where trafficking to its final destination is not dependent on the presence of its TM domains. In the absence of PFE60, MCs are significantly shorter and appear more frequently in a stacked manner. Furthermore, the MC resident protein Pf332 is not correctly trafficked to its final destination in the absence of PFE60. We propose a model where interacting partners (PFE60, Pf332, MAHRP1 and SBP1) might be preassembled on vesicles or buds, which originate from the PVM and eventually form MCs. When, in the presence of PFE60 (Fig. 6 left), vesicles fuse with the forming MC membrane, Pf332 bound to PFE60 acts as a spacer between forming MCs and enables segregation of individual MC lamella. In the absence of PFE60 (Fig. 6 right), Pf332 does not bind to this complex and cannot promote proper segregation. Since REX1 has been described previously to be involved in the segregation process, this protein might be responsible for segregation in some instances but a concerted effort of the two proteins seems to be necessary to achieve complete segregation.

Future analysis of its identified binding partners will help ascertain the complex nature of the malaria parasite virulence complex assembly and might bring us a step closer to combatting this devastating disease.

Acknowledgements

This work was supported by the Australian Research Council (DP1093518 and DP0878953). We thank Anthony Hodder, The Walter and Eliza Hall Institute of Medical Research, Australia, for the gift of Pf332 antibody, Matthew Dixon, Bio21 The University of Melbourne, Australia, for the REX1 antibody, Hans-Peter Beck and Sebastian Rusch, Swiss Tropical and Public Health Institute, Switzerland, for the MAHRP1 antibody, Michael Ryan, La Trobe University, Australia, for the GFP antibody, Jude Przyborski, Philipps-Universitaet Marburg, Germany, for the HSP70x antibody and Klaus Lingelbach, Philipps-Universitaet

564 Marburg, Germany, for the Exp1 antibody. We thank the Australian Red Cross Blood Bank for
565 the gift of red blood cells and human serum. We acknowledge the staff of the Centre for
566 Advanced Microscopy, The Australian National University, Australia, especially Jiwon Lee, for
567 technical support. The Centre for Advanced Microscopy is part of the Australian Microscopy
568 and Microanalysis Research Facility (AMMRF) supported by the National Research
569 Infrastructure, Australia. We would also like to thank Phuong Tran and Tilo Fobes for
570 scientific discussions, Weidong Jing, Erin Andrew and Yingying Hey for technical support with
571 flow cytometry and Sharyn Wragg for the model design.

572

573

References

Arnold, T., Linke, D., 2008. The use of detergents to purify membrane proteins. Curr. Protoc. Protein Sci. 4, 4.8.1–4.8.30. doi:10.1002/0471140864.ps0408s53

Bachmann, A., Scholz, J.A.M., Janßen, M., Klinkert, M.-Q., Tannich, E., Bruchhaus, I., Petter, M., 2015. A comparative study of the localization. Malar. J. 1–18. doi:10.1186/s12936-015-0784-2

Bannister, L.H., Hopkins, J.M., Margos, G., Dluzewski, A.R., Mitchell, G.H., 2004. Three-dimensional ultrastructure of the ring stage of *Plasmodium falciparum*: evidence for export pathways. Microsc. Microanal. 10, 551–562. doi:10.1017/S1431927604040917

Baruch, D.I., Pasloske, B.L., Singh, H.B., Bi, X., Ma, X.C., Feldman, M., Taraschi, T.F., Howard, R.J., 1995. Cloning the *P. falciparum* gene encoding PfEMP1, a malarial variant antigen and adherence receptor on the surface of parasitized human erythrocytes. Cell 82, 77–87.

Beeson, J.G., Brown, G.V., 2002. Pathogenesis of *Plasmodium falciparum* malaria: the roles of parasite adhesion and antigenic variation. Cell. Mol. Life Sci. 59 (2), 258–271.

Benting, J., Mattei, D., Lingelbach, K., 1994. Brefeldin A inhibits transport of the glycophorin-binding protein from *Plasmodium falciparum* into the host erythrocyte. Biochem. J. 300 (Pt 3), 821–826.

Blisnick, T., Morales Betoulle, M.E., Barale, J.C., Uzureau, P., Berry, L., Desroses, S., Fujioka, H., Mattei, D., Braun Breton, C., 2000. Pfsbp1, a Maurer's cleft *Plasmodium falciparum* protein, is associated with the erythrocyte skeleton. Mol. Biochem. Parasitol. 111, 107–121.

Bordier, C., 1981. Phase separation of integral membrane proteins in Triton X-114 solution. J. Biol. Chem. 256, 1604–1607.

Buffet, P.A., Safeukui, I., Deplaine, G., Brousse, V., Prendki, V., Thellier, M., Turner, G.D., Mercereau-Puijalon, O., 2011. The pathogenesis of *Plasmodium falciparum* malaria in humans: insights from splenic physiology. Blood, 117, 381–392. doi:10.1182/blood-2010-04-202911

Caruana, N.J., Cooke, I.R., Faou, P., Finn, J., Hall, N.E., Norman, M., Pineda, S.S., Strugnell, J.M., 2016. A combined proteomic and transcriptomic analysis of slime secreted by the southern bottletail squid, *Sepiadarium austrinum* (Cephalopoda). J Proteomics 148, 170–182. doi:10.1016/j.jprot.2016.07.026

Cox, J., Mann, M., 2008. MaxQuant enables high peptide identification rates, individualized p.p.b.-range mass accuracies and proteome-wide protein quantification. Nat. Biotechnol. 26, 1367–1372. doi:10.1038/nbt.1511

Deponte, M., Hoppe, H.C., Lee, M.C.S., Maier, A.G., Richard, D., Rug, M., Spielmann, T., Przyborski, J.M., 2012. Wherever I may roam: Protein and membrane trafficking in P. falciparum-infected red blood cells. Mol. Biochem. Parasitol. 1–22. doi:10.1016/j.molbiopara.2012.09.007

609 Dixon, M.W.A., Kenny, S., McMillan, P.J., Hanssen, E., Trenholme, K.R., Gardiner, D.L., Tilley,
610 L., 2011. Genetic ablation of a Maurer's cleft protein prevents assembly of the *Plasmodium*
611 *falciparum* virulence complex. Mol. Microbiol. 81, 982–993. doi:10.1111/j.1365-
612 2958.2011.07740.x
613 Dzikowski, R., Frank, M., Deitsch, K., 2006. Mutually exclusive expression of virulence genes by
614 malaria parasites is regulated independently of antigen production. PLoS Pathog 2, e22.
615 doi:10.1371/journal.ppat.0020022
616 Florens, L., Liu, X., Wang, Y., Yang, S., Schwartz, O., Peglar, M., Carucci, D.J., Yates, J.R., III,
617 Wu, Y., 2004. Proteomics approach reveals novel proteins on the surface of malaria-infected
618 erythrocytes. Mol. Biochem. Parasitol. 135, 1–11. doi:10.1016/j.molbiopara.2003.12.007
619 Fujiki, Y., Hubbard, A.L., Fowler, S., Lazarow, P.B., 1982. Isolation of intracellular membranes by
620 means of sodium carbonate treatment: application to endoplasmic reticulum. J. Cell Biol. 93,
621 97–102.
622 Glenister, F.K., Fernandez, K.M., Kats, L.M., Hanssen, E., Mohandas, N., Coppel, R.L., Cooke,
623 B.M., 2009. Functional alteration of red blood cells by a megadalton protein of *Plasmodium*
624 *falciparum*. Blood 113, 919–928. doi:10.1182/blood-2008-05-157735
625 Grüring, C., Heiber, A., Kruse, F., Ungefehr, J., Gilberger, T.-W., Spielmann, T., 2011.
626 Development and host cell modifications of *Plasmodium falciparum* blood stages in four
627 dimensions. Nat Comms 2, 165. doi:10.1038/ncomms1169
628 Günther, K., Tümmler, M., Arnold, H.H., Ridley, R., Goman, M., Scaife, J.G., Lingelbach, K.,
629 1991. An exported protein of *Plasmodium falciparum* is synthesized as an integral membrane
630 protein. Mol. Biochem. Parasitol. 46, 149–157.
631 Haase, S., Herrmann, S., Grüring, C., Heiber, A., Jansen, P.W., Langer, C., Treeck, M., Cabrera, A.,
632 Bruns, C., Struck, N.S., Kono, M., Engelberg, K., Ruch, U., Stunnenberg, H.G., Gilberger, T.-
633 W., Spielmann, T., 2009. Sequence requirements for the export of the *Plasmodium falciparum*
634 Maurer's clefts protein REX2. Mol. Microbiol. 71, 1003–1017. doi:10.1111/j.1365-
635 2958.2008.06582.x
636 Hanssen, E., Hawthorne, P., Dixon, M.W.A., Trenholme, K.R., McMillan, P.J., Spielmann, T.,
637 Gardiner, D.L., Tilley, L., 2008. Targeted mutagenesis of the ring-exported protein-1 of
638 *Plasmodium falciparum* disrupts the architecture of Maurer's cleft organelles. Mol. Microbiol.
639 69, 938–953. doi:10.1111/j.1365-2958.2008.06329.x
640 Hawthorne, P.L., Trenholme, K.R., Skinner-Adams, T.S., Spielmann, T., Fischer, K., Dixon,
641 M.W.A., Ortega, M.R., Anderson, K.L., Kemp, D.J., Gardiner, D.L., 2004. A novel
642 *Plasmodium falciparum* ring stage protein, REX, is located in Maurer's clefts. Mol. Biochem.
643 Parasitol. 136, 181–189.

644 Heiber, A., Kruse, F., Pick, C., Grüring, C., Flemming, S., Oberli, A., Schoeler, H., Retzlaff, S.,
645 Mesén-Ramírez, P., Hiss, J.A., Kadekoppala, M., Hecht, L., Holder, A.A., Gilberger, T.-W.,
646 Spielmann, T., 2013. Identification of new PNEPs indicates a substantial non-PEXEL
647 exportome and underpins common features in *Plasmodium falciparum* protein export. PLoS
648 Pathog 9, e1003546. doi:10.1371/journal.ppat.1003546
649 Hiller, N.L., Bhattacharjee, S., van Ooij, C., Liolios, K., Harrison, T., Lopez-Estraño, C., Haldar,
650 K., 2004. A host-targeting signal in virulence proteins reveals a secretome in malarial infection.
651 Science 306, 1934–1937. doi:10.1126/science.1102737
652 Hodder, A.N., Maier, A.G., Rug, M., Brown, M., Hommel, M., Pantic, I., Puig-de-Morales-
653 Marinkovic, M., Smith, B., Triglia, T., Beeson, J., Cowman, A.F., 2009. Analysis of structure
654 and function of the giant protein Pf332 in *Plasmodium falciparum*. Mol. Microbiol. 71, 48–65.
655 doi:10.1111/j.1365-2958.2008.06508.x
656 Keller, A., Nesvizhskii, A.I., Kolker, E., Aebersold, R., 2002. Empirical statistical model to
657 estimate the accuracy of peptide identifications made by MS/MS and database search. Anal.
658 Chem. 74, 5383–5392.
659 Khattab, A., Klinkert, M.-Q., 2006. Maurer's Clefts-Restricted Localization, Orientation and Export
660 of a *Plasmodium falciparum* RIFIN. Traffic 7, 1654–1665. doi:10.1111/j.1600-
661 0854.2006.00494.x
662 Kilian, N., Dittmer, M., Cyrklaff, M., Ouermi, D., Bisseye, C., Simpore, J., Frischknecht, F.,
663 Sanchez, C.P., Lanzer, M., 2013. Haemoglobin S and C affect the motion of Maurer's clefts in
664 *Plasmodium falciparum*-infected erythrocytes. Cell. Microbiol. 15, 1111–1126.
665 doi:10.1111/cmi.12102
666 Knuepfer, E., Rug, M., Klonis, N., Tilley, L., Cowman, A.F., 2005. Trafficking of the major
667 virulence factor to the surface of transfected *P. falciparum*-infected erythrocytes. Blood 105,
668 4078–4087. doi:10.1182/blood-2004-12-4666
669 Külzer, S., Charnaud, S., Dagan, T., Riedel, J., Mandal, P., Pesce, E.R., Blatch, G.L., Crabb, B.S.,
670 Gilson, P.R., Przyborski, J.M., 2012. *Plasmodium falciparum*-encoded exported hsp70/hsp40
671 chaperone/co-chaperone complexes within the host erythrocyte. Cell. Microbiol. 14, 1784–
672 1795. doi:10.1111/j.1462-5822.2012.01840.x
673 Külzer, S., Rug, M., Brinkmann, K., Cannon, P., Cowman, A., Lingelbach, K., Blatch, G.L., Maier,
674 A.G., Przyborski, J.M., 2010. Parasite-encoded Hsp40 proteins define novel mobile structures
675 in the cytosol of the *P. falciparum*-infected erythrocyte. Cell. Microbiol. 12, 1398–1420.
676 doi:10.1111/j.1462-5822.2010.01477.x
677 Lambros, C., Vanderberg, J.P., 1979. Synchronization of *Plasmodium falciparum* erythrocytic
678 stages in culture. J Parasitol, 65, 418–420.

679 Langreth, S.G., Jensen, J.B., Reese, R.T., Trager, W., 1978. Fine structure of human malaria in
680 vitro. J. Protozool. 25, 443–452.
681 Maier, A.G., Cooke, B.M., Cowman, A.F., Tilley, L., 2009. Malaria parasite proteins that remodel
682 the host erythrocyte. Nat. Rev. Microbiol. 7, 341–354. doi:10.1038/nrmicro2110
683 Maier, A.G., Rug, M., 2013. In vitro culturing *Plasmodium falciparum* erythrocytic stages, in:
684 Ménard, R. (Ed.), Malaria: Methods and Protocols. Humana Press, US, pp 3–15.
685 doi:10.1007/978-1-62703-026-7_1
686 Maier, A.G., Rug, M., O'Neill, M.T., Brown, M., Chakravorty, S., Szestak, T., Chesson, J., Wu, Y.,
687 Hughes, K., Coppel, R.L., Newbold, C., Beeson, J.G., Craig, A., Crabb, B.S., Cowman, A.F.,
688 2008. Exported proteins required for virulence and rigidity of *Plasmodium falciparum*-infected
689 human erythrocytes. Cell 134, 48–61. doi:10.1016/j.cell.2008.04.051
690 Marti, M., Good, R.T., Rug, M., Knuepfer, E., Cowman, A.F., 2004. Targeting malaria virulence
691 and remodeling proteins to the host erythrocyte. Science 306, 1930–1933.
692 doi:10.1126/science.1102452
693 Mundwiler-Pachlatko, E., Beck, H.-P., 2013. Maurer's clefts, the enigma of *Plasmodium*
694 *falciparum*. PNAS 110, 19987–19994. doi:10.1073/pnas.1309247110
695 Nesvizhskii, A.I., Keller, A., Kolker, E., Aebersold, R., 2003. A statistical model for identifying
696 proteins by tandem mass spectrometry. Anal. Chem. 75, 4646–4658.
697 Nilsson, S., Angeletti, D., Wahlgren, M., Chen, Q., Moll, K., 2012. *Plasmodium falciparum* antigen
698 332 is a resident peripheral membrane protein of Maurer's clefts. PLoS ONE 7, e46980.
699 doi:10.1371/journal.pone.0046980
700 Oberli, A., Slater, L.M., Cutts, E., Brand, F., Mundwiler-Pachlatko, E., Rusch, S., Masik, M.F.G.,
701 Erat, M.C., Beck, H.-P., Vakonakis, I., 2014. A *Plasmodium falciparum* PHIST protein binds
702 the virulence factor PfEMP1 and comigrates to knobs on the host cell surface. FASEB J. 28,
703 4420–4433. doi:10.1096/fj.14-256057
704 Pasloske, B.L., Baruch, D.I., van Schravendijk, M.R., Handunnetti, S.M., Aikawa, M., Fujioka, H.,
705 Taraschi, T.F., Gormley, J.A., Howard, R.J., 1993. Cloning and characterization of a
706 *Plasmodium falciparum* gene encoding a novel high-molecular weight host membrane-
707 associated protein, PfEMP3. Mol. Biochem. Parasitol. 59, 59–72.
708 Pesce, E.-R., Acharya, P., Tatu, U., Nicoll, W.S., Shonhai, A., Hoppe, H.C., Blatch, G.L., 2008.
709 The *Plasmodium falciparum* heat shock protein 40, Pfj4, associates with heat shock protein 70
710 and shows similar heat induction and localisation patterns. Int. J. Biochem. Cell Biol. 40, 2914–
711 2926. doi:10.1016/j.biocel.2008.06.011
712 Przyborski, J., Miller, S.K., Pfahler, J.M., Henrich, P.P., Rohrbach, P., Carbb, B.S., Lanzer, M.,
713 2005. Trafficking of STEVOR to the Maurer's clefts in *Plasmodium falciparum*-infected

714 erythrocytes. EMBO J. 24, 2306–2317.
715 Regev-Rudzki, N., Wilson, D.W., Carvalho, T.G., Sisquella, X., Coleman, B.M., Rug, M., Bursac,
716 D., Angrisano, F., Gee, M., Hill, A.F., Baum, J., Cowman, A.F., 2013. Cell-Cell
717 Communication between Malaria-Infected Red Blood Cells via Exosome-like Vesicles. Cell
718 153, 1120–1133. doi:10.1016/j.cell.2013.04.029
719 Rug, M., Cyrklaff, M., Mikkonen, A., Lemgruber, L., Kuelzer, S., Sanchez, C.P., Thompson, J.,
720 Hanssen, E., O'Neill, M., Langer, C., Lanzer, M., Frischknecht, F., Maier, A.G., Cowman, A.F.,
721 2014. Export of virulence proteins by malaria-infected erythrocytes involves remodeling of host
722 actin cytoskeleton. Blood 124, 3459–3468. doi:10.1182/blood-2014-06-583054
723 Rug, M., Maier, A.G., 2013. Transfection of *Plasmodium falciparum*, in: Ménard, R. (Ed.),
724 Malaria: Methods and Protocols. Humana Press, US, 75-98.
725 Rug, M., Wickham, M.E., Foley, M., Cowman, A.F., Tilley, L., 2004. Correct promoter control is
726 needed for trafficking of the ring-infected erythrocyte surface antigen to the host cytosol in
727 transfected malaria parasites. Infect. Immun. 72, 6095–6105. doi:10.1128/IAI.72.10.6095-
728 6105.2004
729 Salanti, A., Dahlbäck, M., Turner, L., Nielsen, M.A., Barfod, L., Magistrado, P., Jensen, A.T.R.,
730 Lavstsen, T., Ofori, M.F., Marsh, K., Hviid, L., Theander, T.G., 2004. Evidence for the
731 involvement of VAR2CSA in pregnancy-associated malaria. J. Exp. Med. 200, 1197–1203.
732 doi:10.1084/jem.20041579
733 Sam-Yellowe, T., Florens, L., Johnson, J.R., Wang, T., Drazba, J.A., Le Roch, K.G., Zhou, Y.,
734 Batalov, S., Carucci, D.J., Winzeler, E.A., Yates, J.R., III, 2004. A *Plasmodium* gene family
735 encoding Maurer's celft membrane proteins: Structural properties and Expression Profiling.
736 Genome Res 14, 1052–1059. doi:10.1101/gr.2126104
737 Sam-Yellowe, T.Y., 2009. The role of the Maurer's clefts in protein transport in *Plasmodium*
738 *falciparum*. Trends Parasitol, 25, 277–284. doi:10.1016/j.pt.2009.03.009
739 Sargeant, T.J., Marti, M., Caler, E., Carlton, J.M., Simpson, K., Speed, T.P., Cowman, A.F., 2006.
740 Lineage-specific expansion of proteins exported to erythrocytes in malaria parasites. Genome
741 Biol. 7, R12. doi:10.1186/gb-2006-7-2-r12
742 Saridaki, T., Fröhlich, K.S., Braun-Breton, C., Lanzer, M., 2009. Export of PfSBP1 to the
743 *Plasmodium falciparum* Maurer's Clefts. Traffic 10, 137–152. doi:10.1111/j.1600-
744 0854.2008.00860.x
745 Schook, W., Puszkin, S., Bloom, W., Ores, C., Kochwa, S., 1979. Mechanochemical properties of
746 brain clathrin: interactions with actin and alpha-actinin and polymerization into basketlike
747 structures or filaments. Proc. Natl. Acad. Sci. U.S.A. 76, 116–120.
748 Silva, J.C., Gorenstein, M.V., Li, G.-Z., Vissers, J.P.C., Geromanos, S.J., 2006. Absolute

quantification of proteins by LCMSE: a virtue of parallel MS acquisition. Mol. Cell Proteomics 5, 144–156. doi:10.1074/mcp.M500230-MCP200

Singh, A.P., Buscaglia, C.A., Wang, Q., Levay, A., Nussenzweig, D.R., Walker, J.R., Winzeler, E.A., Fujii, H., Fontoura, B.M.A., Nussenzweig, V., 2007. *Plasmodium* circumsporozoite protein promotes the development of the liver stages of the parasite. Cell 131, 492–504. doi:10.1016/j.cell.2007.09.013

Smith, J.D., Craig, A.G., Kriek, N., Hudson-Taylor, D., Kyes, S., Fagan, T., Fagen, T., Pinches, R., Baruch, D.I., Newbold, C.I., Miller, L.H., 2000. Identification of a *Plasmodium falciparum* intercellular adhesion molecule-1 binding domain: a parasite adhesion trait implicated in cerebral malaria. Proc. Natl. Acad. Sci. U.S.A. 97, 1766–1771. doi:10.1073/pnas.040545897

Spielmann, T., Hawthorne, P.L., Dixon, M.W.A., Hannemann, M., Klotz, K., Kemp, D.J., Klonis, N., Tilley, L., Trenholme, K.R., Gardiner, D.L., 2006. A cluster of ring stage-specific genes linked to a locus implicated in cytoadherence in *Plasmodium falciparum* codes for PEXEL-negative and PEXEL-positive proteins exported into the host cell. Mol. Biol. Cell 17, 3613–3624. doi:10.1091/mbc.E06-04-0291

Spycher, C., Klonis, N., Spielmann, T., Kump, E., Steiger, S., Tilley, L., Beck, H.-P., 2003. MAHRP-1, a novel *Plasmodium falciparum* histidine-rich protein, binds ferriprotoporphyrin IX and localizes to the Maurer's clefts. J. Biol. Chem. 278, 35373–35383. doi:10.1074/jbc.M305851200

Su, X.Z., Heatwole, V.M., Wertheimer, S.P., Guinet, F., Herrfeldt, J.A., Peterson, D.S., Ravetch, J.A., Wellems, T.E., 1995. The large diverse gene family var encodes proteins involved in cytoadherence and antigenic variation of *Plasmodium falciparum*-infected erythrocytes. Cell 82, 89–100.

Tran, P.N., Brown, S.H.J., Mitchell, T.W., Matuschewski, K., McMillan, P.J., Kirk, K., Dixon, M.W.A., Maier, A.G., 2014. A female gametocyte-specific ABC transporter plays a role in lipid metabolism in the malaria parasite. Nat Comms 5, 4773. doi:10.1038/ncomms5773

Vincensini, L., Fall, G., Berry, L., Blisnick, T., Braun-Breton, C., 2008. The RhopH complex is transferred to the host cell cytoplasm following red blood cell invasion by *Plasmodium falciparum*. Mol. Biochem. Parasitol. 160, 81–89. doi:10.1016/j.molbiopara.2008.04.002

Vincensini, L., Richert, S., Blisnick, T., Van Dorsselaer, A., Leize-Wagner, E., Rabilloud, T., Braun-Breton, C., 2005. Proteomic analysis identifies novel proteins of the Maurer's clefts, a secretory compartment delivering *Plasmodium falciparum* proteins to the surface of its host cell. Mol. Cell Proteomics 4, 582–593. doi:10.1074/mcp.M400176-MCP200

Voss, T.S., Healer, J., Marty, A.J., Duffy, M.F., Thompson, J.K., Beeson, J.G., Reeder, J.C., Crabb, B.S., Cowman, A.F., 2006. A var gene promoter controls allelic exclusion of virulence genes in

Plasmodium falciparum malaria. Nature 439, 1004–1008. doi:10.1038/nature04407

Waller, K.L., Stubberfield, L.M., Dubljevic, V., Nunomura, W., An, X., Mason, A.J., Mohandas, N., Cooke, B.M., Coppel, R.L., 2007. Interactions of *Plasmodium falciparum* erythrocyte membrane protein 3 with the red blood cell membrane skeleton. Biochim. Biophys. Acta 1768, 2145–2156. doi:10.1016/j.bbamem.2007.04.027

Waterkeyn, J.G., Cowman, A.F., Cooke, B.M., 2001. *Plasmodium falciparum*: gelatin enrichment selects for parasites with full-length chromosome 2. implications for cytoadhesion assays. Exp. Parasitol. 97, 115–118. doi:10.1006/expr.2000.4593

Waterkeyn, J.G., Wickham, M.E., Davern, K.M., Cooke, B.M., Coppel, R.L., Reeder, J.C., Culvenor, J.G., Waller, R.F., Cowman, A.F., 2000. Targeted mutagenesis of *Plasmodium falciparum* erythrocyte membrane protein 3 (PfEMP3) disrupts cytoadherence of malaria-infected red blood cells. EMBO J. 19, 2813–2823. doi:10.1093/emboj/19.12.2813

Wickham, M.E., Rug, M., Ralph, S.A., Klonis, N., McFadden, G.I., Tilley, L., Cowman, A.F., 2001. Trafficking and assembly of the cytoadherence complex in *Plasmodium falciparum*-infected human erythrocytes. EMBO J. 20, 5636–5649. doi:10.1093/emboj/20.20.5636

Winter, G., Kawai, S., Haeggström, M., Kaneko, O., Euler, von, A., Kawazu, S.-I., Palm, D., Fernandez, V., Wahlgren, M., 2005. SURFIN is a polymorphic antigen expressed on *Plasmodium falciparum* merozoites and infected erythrocytes. J. Exp. Med. 201, 1853–1863. doi:10.1084/jem.20041392

Xie, Y., Zheng, Y., Li, H., Luo, X., He, Z., Cao, S., Shi, Y., Zhao, Q., Xue, Y., Zuo, Z., Ren, J., 2016. GPS-Lipid: a robust tool for the prediction of multiple lipid modification sites. Sci Rep 6, 28249. doi:10.1038/srep28249

Figure legends

Fig. 1. *Plasmodium falciparum* export protein PFE60 is a resident Maurer's cleft (MC) protein not exposed on the infected red blood cell (iRBC) surface. (A) Histogram of flow cytometric analysis of live and permeabilised PFE60-GFP iRBCs (20-28 h post invasion). (a) Live PFE60-GFP iRBCs labelled with anti-PFE60 antibody (blue curve) showed a similar fluorescent background level as live cells without antibody labeling (negative control; red curve); (b) permeabilised PFE60-GFP iRBCs demonstrated clear labeling of the internal PFE60 protein pool with anti-PFE60 antibody (positive control; blue curve) in contrast to unlabeled permeabilised cells (red curve); (c) live PFE60-GFP iRBCs were labeled with anti-glycophorin C antibody as a positive control for a surface-exposed protein (blue curve) and compared with no antibody treatment (red curve). (B) Dual immunofluorescence assays of PFE60 with exported proteins localized in different areas of the iRBC. CS2WT or PFE60-hemagglutinin (HA)/Strep iRBCs were probed with anti-PFE60 (or anti-HA) (first column), and co-localisation studies carried out with anti- *P. falciparum* Exported Membrane Protein 3 (PfEMP3), anti-*Plasmodium* Transport Protein 2 (PTP2), anti-Heat Shock Protein 70x (HSP70x), anti-PTP1 and anti-skeleton-binding protein 1 (SBP1) (second column). PFE60 strongly co-localises with the MC resident proteins SBP1 and PTP1. The 'Overlay' column shows an overlay of the two fluorescence signals and merged images of the fluorescence signal, DAPI and bright field are depicted in the 'Merge' column. Scale bar: 4 μm. (C) Trypsin treatment of live PFE60-GFP iRBCs (20-28 h post invasion). The same punctate GFP signal was observed in trypsin treated iRBCs as in untreated cells indicating that PFE60 is not exposed on the surface of iRBC. (- tryp) untreated cells; (+ tryp) trypsin treated cells; (+ tryp/PMSF) cells treated with trypsin plus protease inhibitor phenylmethane sulfonyl fluoride. The 'PFE60-GFP' column shows the fluorescence signal and the 'Merge' column shows the overlay of the fluorescence signal and the bright field image. Scale bar: 4 μm. (D) Western blot analysis of trypsin-treated PFE60-GFP iRBCs (20-28 h post invasion). The full-

836 length PFE60-GFP was detected using antibodies recognising the N-terminus (anti-PFE60)
837 and C-terminus (anti-GFP) of PFE60-GFP, indicating no cleavage had taken place. *Plasmodium*
838 *falciparum* erythrocyte membrane protein 1 (PfEMP1) was used as a positive control for
839 cleavage upon surface exposure. The full-length protein (internal pool of PfEMP1; >300 kDa)
840 and the cytoplasmic tail of the surface-exposed pool of PfEMP1 (70 kDa and 90 kDa) were
841 detected using anti-ATS antibodies. Uninfected RBCs (uRBC) were used to distinguish PfEMP1
842 from cross-reactive RBC proteins.
843
844 **Fig. 2.** The transmembrane (TM) domains of *Plasmodium falciparum* export protein PFE60
845 are required for integration of PFE60 into the Maurer's cleft (MC) membrane but are not
846 essential for its trafficking to the organelle. (A) Schematic representation of the protein
847 structure of PFE60, PFE60-GFP and PFE60ΔTM-GFP drawn to scale. PEXEL, *Plasmodium*
848 export element; VTS, vacuolar transport signal. (B) PFE60-GFP and PFE60ΔTM–GFP localise
849 to punctate structures in the infected red blood cell (iRBC) cytoplasm. GFP signal in live iRBCs
850 expressing full-length PFE60-GFP and PFE60ΔTM–GFP in different stages of the asexual life
851 cycle (Ring, ring stage; Troph, trophozoite stage; Schiz, schizont stage). The fluorescence
852 signal is depicted on the left and the overlay of the fluorescence signal and bright field images
853 on the right of each panel. Scale bar: 4 μm. (C) PFE60-GFP, PFE60ΔTM-GFP and
854 ΔPFE60/PFE60-GFP(comp) all co-localise with the MC resident protein PTP1 in *Plasmodium*
855 *falciparum* iRBCs. Immunofluorescence assays with anti-GFP (GFP) and anti-PTP1 (PTP1)
856 show overlap of the two signals in all three cell lines (Overlay) and the 'Merge' depicts merged
857 images of the fluorescence signal, DAPI and bright field. Scale bar: 4 μm. (D) PFE60-GFP is an
858 integral membrane protein whereas PFE60ΔTM-GFP is a peripheral membrane protein.
859 Magnet purified PFE60-GFP and PFE60ΔTM-GFP iRBCs (20-28 h post invasion) were
860 separated with Triton X-114 into aqueous (A) and detergent (D) phases. Hypotonically lysed
861 cells were treated with Na_2CO_3 (pH11.5) or urea; samples were then separated into

862 supernatant (S) and pellet (P) fractions and subjected to SDS-PAGE. In subsequent western
863 blot analysis, the membranes were probed with anti-GFP antibody, stripped and re-probed
864 with anti-PFD1170c (control for peripheral membrane protein) and anti-Exp1 antibody
865 (control for integral membrane protein).
866
867 **Fig. 3.** Phenotypical analysis of *Plasmodium falciparum* export protein ΔPFE60 cells. (A) The
868 Maurer's cleft (MC) resident protein Pf332 is not correctly trafficked in the absence of PFE60.
869 Trafficking of MC resident proteins PTP1, SBP1, REX1 and MAHRP1 is not altered in ΔPFE60
870 versus wild type (WT) infected red blood cells (iRBCs) whereas Pf332 is localized to punctate
871 areas distinct from the MCs. WT depicts IFA images of the WT cell line and ΔPFE60 images of
872 the ΔPFE60 cell line. FP, Fluorescence pattern with respective antibodies; overlay, overlay of
873 the fluorescence, with DAPI (to indicate nuclear location) and brightfield images. Scale bar: 4
874 μm. (B) Deletion of PFE60 does not cause significant changes in the surface morphology of
875 *Plasmodium falciparum* iRBCs. The surface of uninfected RBCs (uRBC), WT and ΔPFE60 iRBCs
876 was studied by scanning electron microscopy. Uninfected RBCs display a smooth surface
877 whereas WT and ΔPFE60 iRBCs show similar protrusions (knobs) all over their surface. Scale
878 bar: 2 μm. Each image is representative of >20 studied cells.
879
880 **Fig. 4.** The Maurer's cleft (MC) architecture is significantly different in the absence of
881 *Plasmodium falciparum* export protein PFE60. (A) Expression pattern of PFE60-GFP and
882 ΔPFE60/PFE60-GFP(comp) is similar throughout the *Plasmodium falciparum* asexual life
883 cycle, verifying correct expression timing in ΔPFE60/PFE60-GFP(comp). Western blot
884 analysis shows expression of a 70 kDa protein from late rings to early schizonts in both cell
885 lines (equal numbers of tightly synchronized infected red blood cells (iRBCs) were taken at 6
886 h intervals). *Plasmodium falciparum* Heat Shock Protein 70 (PfHSP70) was used as a loading
887 control. (B) PFE60 plays a role in the architecture of MCs. Transmission electron microscopy

888 of single MC lamellae in a wild type (WT) RBC (a) versus stacked MCs in a ΔPFE60 iRBC (b).
889 (C) ΔPFE60 iRBCs display a significantly higher number of stacked Maurer's clefts than WT
890 iRBCs. Three biological replicates were used; each replicate represents an independent
891 experiment; 30 randomly chosen MCs were counted in each replicate; >80 cells were
892 examined for each cell line. The knock-out phenotype is reverted in ΔPFE60/PFE60-
893 GFP(comp) iRBC. $P>0.05$, ** $P<0.01$, *** $P<0.001$, NS, not significant. (D) The average length of
894 MCs is significantly shorter in ΔPFE60 iRBCs versus WT iRBCs. Three biological replicates
895 were used; each replicate represents an independent experiment with >30 randomly chosen
896 MCs in each replicate; >80 cells were examined for each cell line. $P>0.05$, ** $P<0.01$, ***
897 $P<0.001$.
898
899 **Fig. 5.** *Plasmodium falciparum* export protein PFE60 interacts with the Maurer's cleft (MC)
900 resident protein SBP1. (A) Pull down assays on PFE60-haemagglutinin (HA)/Strep versus a
901 wild type (WT) cell line performed on anti-HA coupled beads. A protein of the expected
902 molecular weight for PFE60-HA/Strep was only detected in the eluate of the bound fraction
903 after western blot analysis with anti-HA antibody. No protein could be detected in the WT cell
904 line or in the flow-through fractions. When stripped and re-probed with anti-SBP1 antibody, a
905 band of the expected size for SBP1 was detected in the eluate of the PFE60-HA/Strep bound
906 fraction implying interaction of the two proteins. (B) Reciprocal immunoprecipitation assays
907 confirm an interaction of PFE60 and SBP1. PFE60 antibody- (a) or SBP1 antibody- (b) loaded
908 beads were incubated with WT infected red blood cells (iRBCs) and interacting proteins were
909 determined after immunoprecipitation by western blot analysis probed with the reciprocal
910 antibodies. Normal rabbit serum (NRS) was used as a control to verify specific binding of
911 interacting partners.
912

Fig. 6. Proposed model outlining the interaction and function of Maurer's cleft (MC) proteins involved in MC segregation. Interacting partners (*Plasmodium falciparum* export protein (PFE60), Pf332, MAHRP1 and SBP1) might be preassembled on vesicles or buds, which originate from the parasitophorous vacuole membrane (PVM) and continue on to form MCs. Pf332 bound to PFE60 acts as a spacer between forming MCs and enables segregation of individual MC lamella in the presence of PFE60 (WT, wild type). In the absence of PFE60 (ΔPFE60), Pf332 does not bind to this complex and cannot promote proper segregation. REX1 might be involved in the segregation process, but the two proteins seem to be necessary to achieve complete segregation.

Supplementary Figure legends

Supplementary Fig. S1. Strategies used to create (A) PFE60-GFP, (B) PFE60ΔTM-GFP, (C) ΔPFE60/PFE60-GFP(comp) *Plasmodium falciparum* cell lines and (D) PFE60-HA/Strep. Vectors pGREP-1 and pHAST-1 were used for integration and expression from the endogenous gene locus and pGLUX-6 for episomal expression (Rug and Maier, 2013). WT, wild type; hDHFR, human dihydrofolate reductase; PAC, puromycin N-acetyltransferase; UTR, untranslated region.

Reference

Rug, M., Maier, A.G., 2013. Transfection of *Plasmodium falciparum*, in: Ménard, R. (Ed.), Malaria: Methods and Protocols. Humana Press, US, 75-98.

Supplementary Fig. S2. Solubility profile of *Plasmodium falciparum* export protein PFE60 and analysis of the consequences of its absence in the asexual life cycle. (A) Carbonate extraction profile of *P. falciparum* export protein PFE60 does not change throughout the

939 asexual life cycle. Ring, trophozoite and schizont stage PFE60-GFP infected red blood cells
940 (iRBCs) were hypotonically lysed and treated with Na_2CO_3 (pH11.5); samples were then
941 separated into supernatant (S) and pellet (P) fractions and subjected to SDS-PAGE. In
942 subsequent western blot analyses, the membranes were probed with anti-GFP antibody,
943 stripped and re-probed with anti-Exp1 antibody (control for integral membrane protein). (B)
944 Deletion of PFE60 does not interrupt trafficking of exported proteins HSP70x, PfEMP1 and
945 PfEMP3 to Maurer's clefts (MCs). Wild type (WT) or ΔPFE60 iRBCs were probed with anti-
946 HSP70x, anti-PfEMP1 or anti-PfEMP3 in immunofluorescence assays. Both panels show the
947 fluorescence signal in the first column and the overlay of the fluorescence signal, DAPI and
948 bright field images in the second column. Scale bar: 4 μm. Each image is representative of 20
949 captured images. (C) Co-labeling of a known MC marker (REX1) with Pf332 in WT versus
950 ΔPFE60 iRBCs. Immunofluorescence assay co-labeling of cells with REX1 and Pf332 revealed
951 that Pf332 does not localise to MCs in ΔPFE60 iRBCs (lower panel overlay) in comparison
952 with WT cells where both REX1 and Pf332 display a co-localisation pattern (upper panel
953 overlay). The first image in both panels shows the signal from the REX1 antibody, the second
954 image the signal from the Pf332 antibody, the third panel the overlay of the two fluorescent
955 images and the fourth image the overlay of fluorescence with bright field and DAPI image.
956 Scale bar: 4 μm. (D) Pf332 average integrated fluorescence density is significantly reduced in
957 ΔPFE60 iRBCs. A two-tailed t-test (unpaired) was conducted to compare Pf332 and REX1
958 labeling in an immunofluorescence assay. The fluorescence signal for Pf332 was significantly
959 reduced in WT versus ΔPFE60 iRBCs whereas no significant difference could be observed for
960 REX1 labeling in the same co-localisation experiment. Mean ± S.E.M. of REX1 in WT 141,700 ±
961 7373, n=28; mean ± S.E.M. of REX1 in PFE60KO 125,500 ± 9299, n=28; P >0.05; NS, not
962 significant. Mean ± S.E.M. of Pf332 in WT 174,200 ± 12560, n=28; mean ± S.E.M. of Pf332 in
963 PFE60KO 88,730 ± 8867, n=28; P <0.0001; ***,significant. (E) Number of punctae is reduced
964 in ΔPFE60 iRBC. The number of punctae representative of MCs was counted in both ΔPFE60

and WT iRBCs on an immunofluorescence assay labeled with anti-REX1 antibody. The average numbers of punctae/cell were plotted and reveal a slightly lower number in ΔPFE60 versus WT iRBCs. An unpaired two-tailed t-test was conducted to compare the average number of REX1 fluorescence labeled punctae in WT versus ΔPFE60 iRBCs. Mean ± S.E.M. of REX1 labeled punctae in WT 19.00 ± 0.8471, n=3; mean ± S.E.M. of REX1 labeled punctae in ΔPFE60 iRBCs 16.65 ± 0.9215, n=37; P>0.05; NS, not significant. (F) Protein expression of PFE60 in WT, ΔPFE60 and ΔPFE60/PFE60-GFP(comp) cell lines (20-28 h post invasion). Saponin lysed WT and ΔPFE60/PFE60-GFP(comp) cell lines show the expected masses in western blot analyses, probed with anti-PFE60 antibody, and the absence thereof in the ΔPFE60 cell line. The blot was stripped and re-probed with anti-Exp1 antibody to verify equal loading.

976

Table 1. Identification of interacting partners of *Plasmodium falciparum* export protein PFE60 via pull down assay and subsequent MS analysis. Pull down of interacting partners was performed on a PFE60- hemagglutinin (HA)/Strep cell line with anti-HA coupled beads. Bound fractions were eluted from the column and subjected to identification by MS analysis. Two independent experiments and analyses were performed with the wild type (WT) cell line as a control. The table shows the top five PFE60-HA/Strep cell line-specific protein hits identified, ranked by their quantity value obtained by the MS analysis (quantity value > 1.00E+07 in both pull down experiments).

Identified Proteins	Gene name	UniProt. Accession Number	Molecular Weight (kDa)	Unique Peptide Pull down 1	Ur
PIESP2 erythrocyte surface protein	PFE0060w PF3D7_0501200	Q8I488_PLAF7	49	16	
Antigen 332, DBL-like protein	PF332 PF3D7_1149000	Q8IHN4_PLAF7	689	15	
Skeleton-binding protein 1	PfSBP1 PF3D7_0501300	Q8I487_PLAF7	36	4	
Membrane associated histidine-rich protein	MAHRP1 PF3D7_1370300	C0H5L9_PLAF7	29	5	
Putative un-characterized protein	PFE0050w PF3D7_0501000	Q8I490_PLAF7	31	4	

977

Figure 1

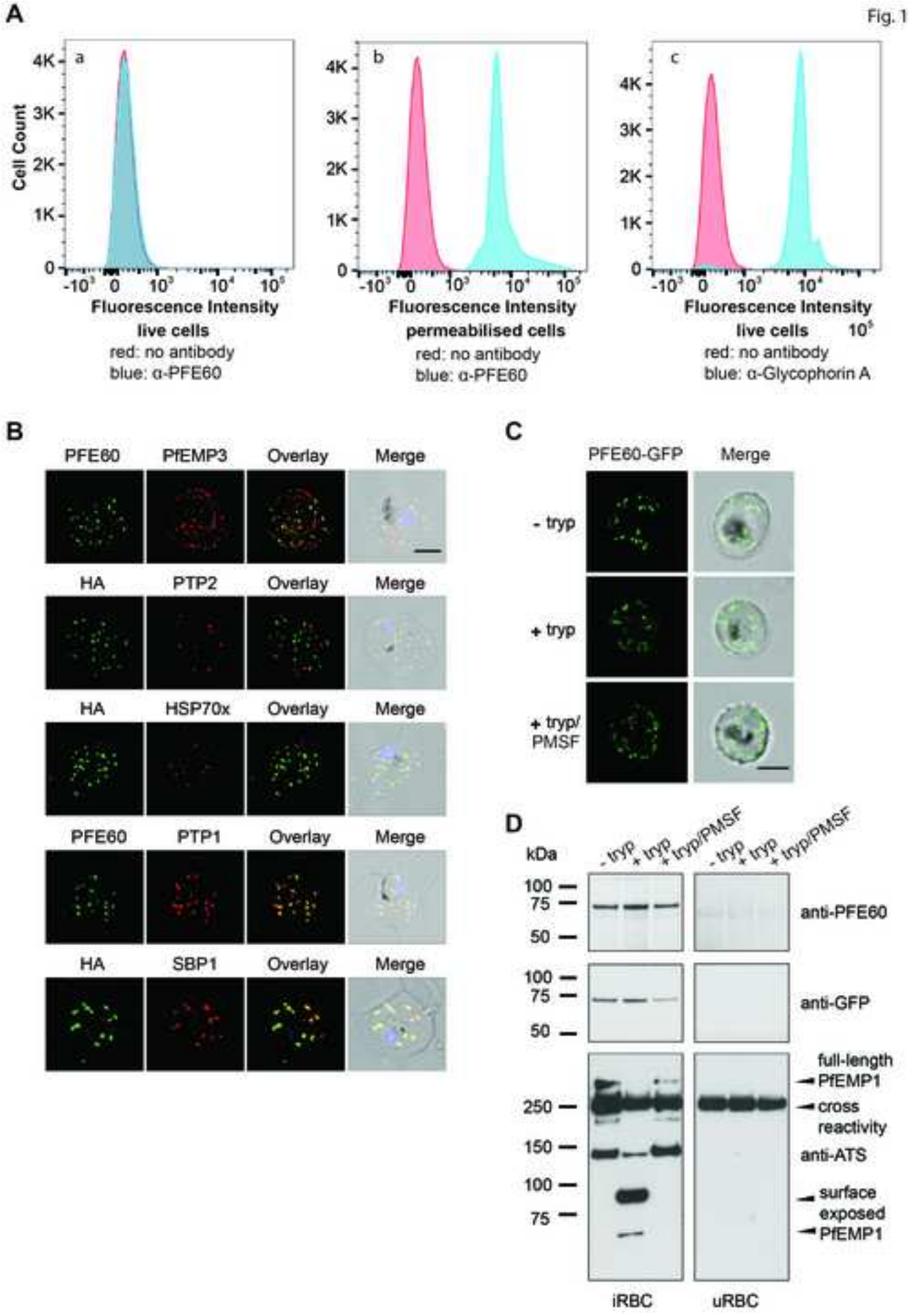

Figure 2

Fig. 2

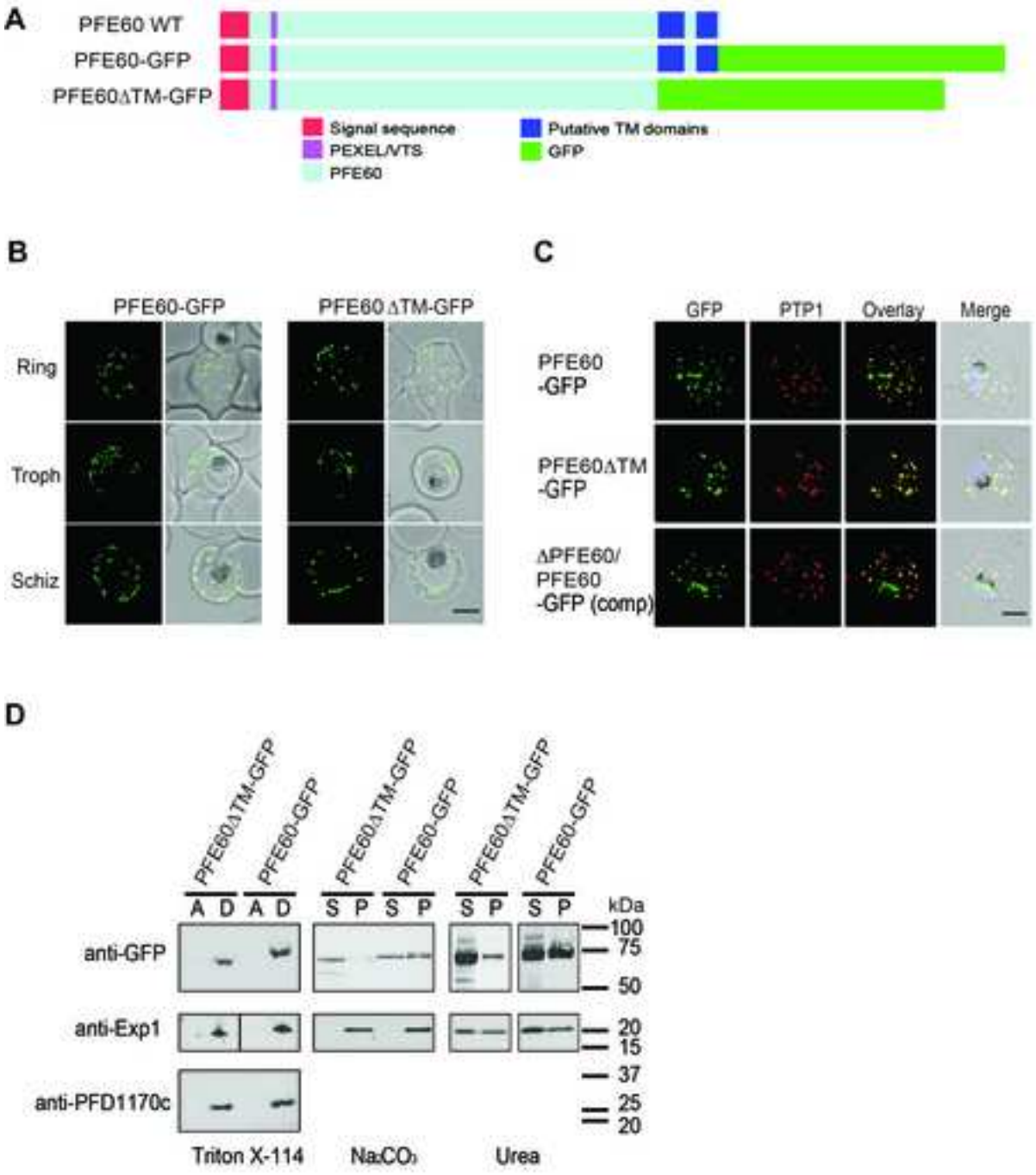

Figure 3

Fig. 3

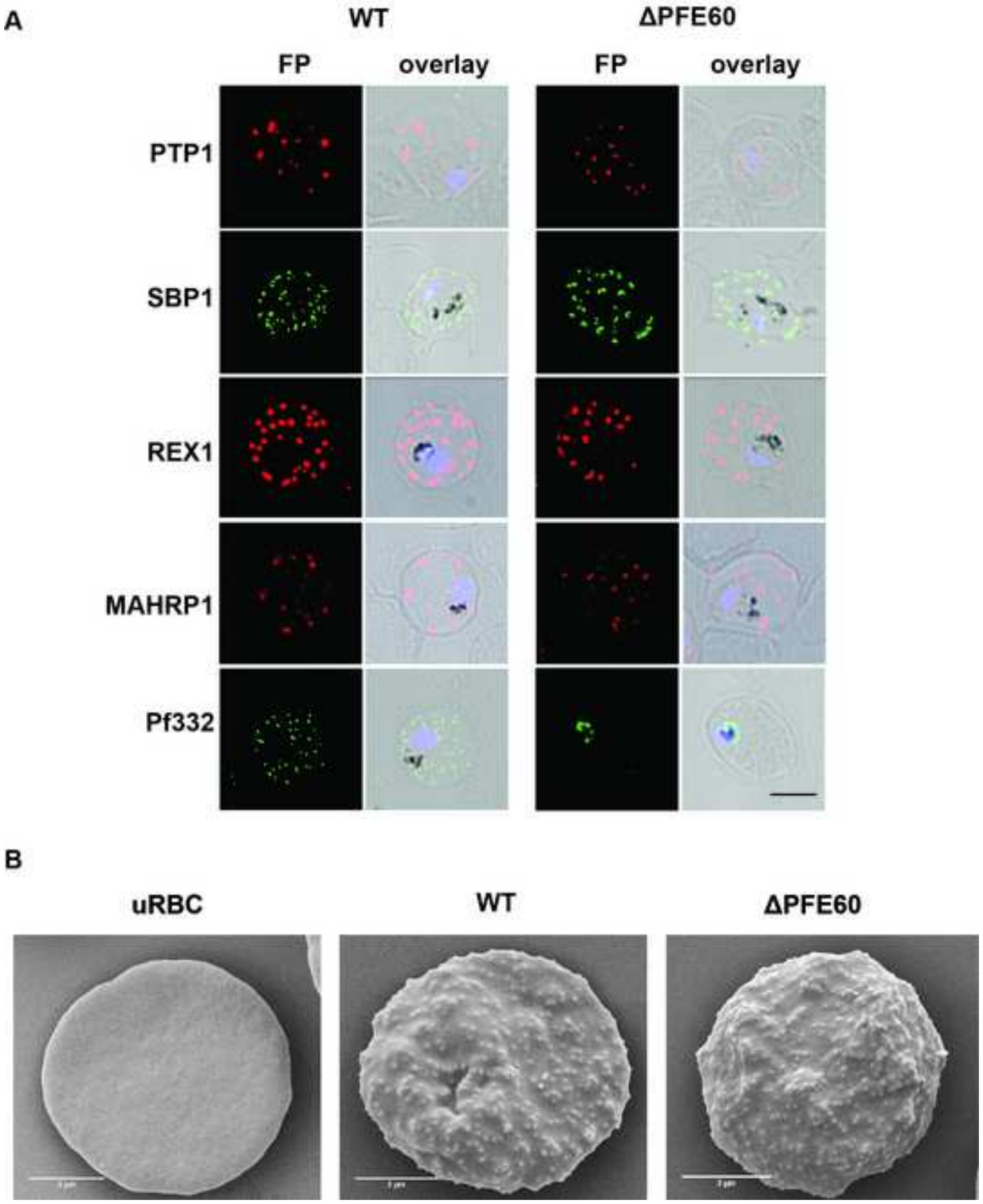

Figure 4

Fig. 4

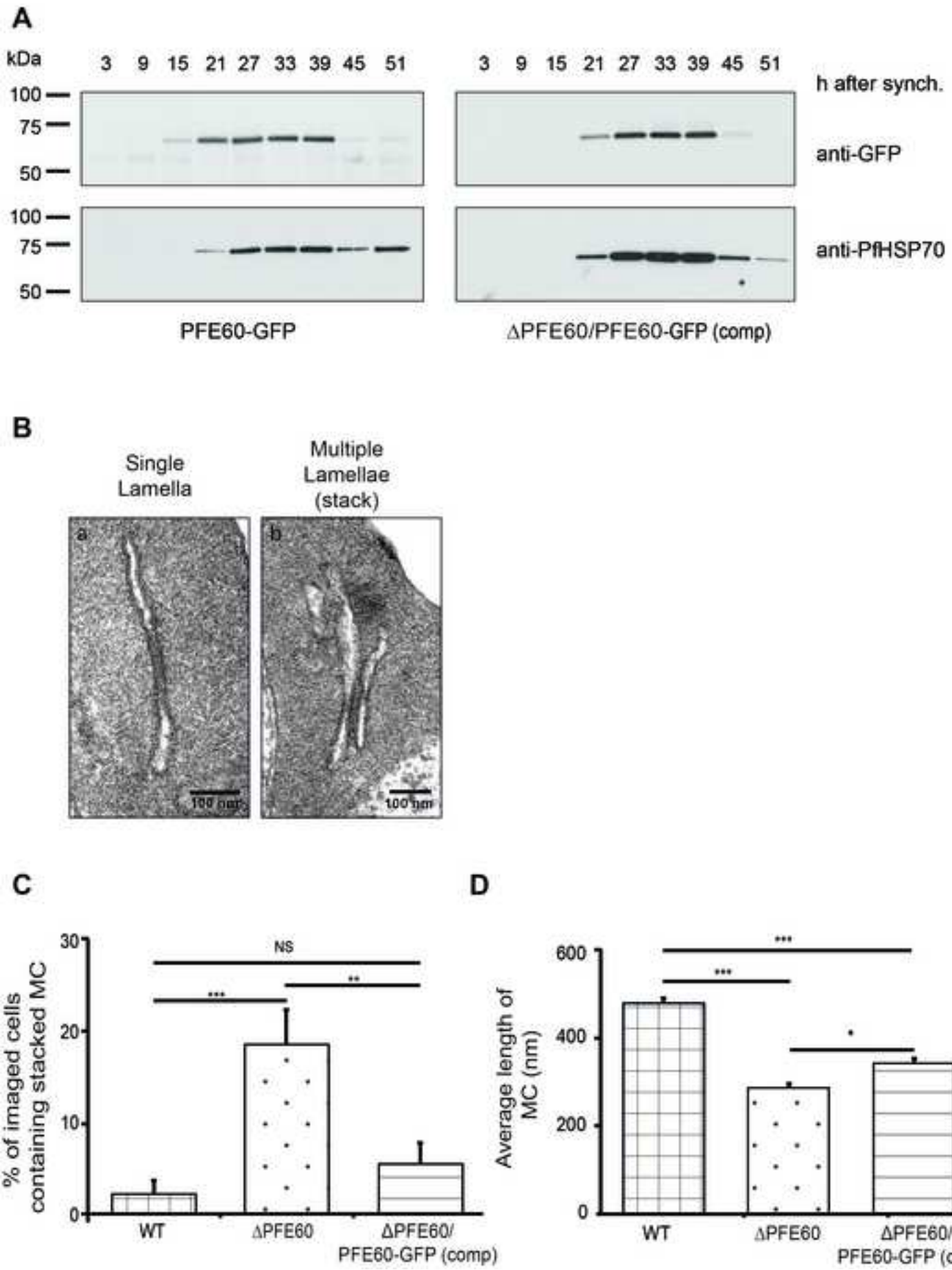

Figure 5

Fig. 5

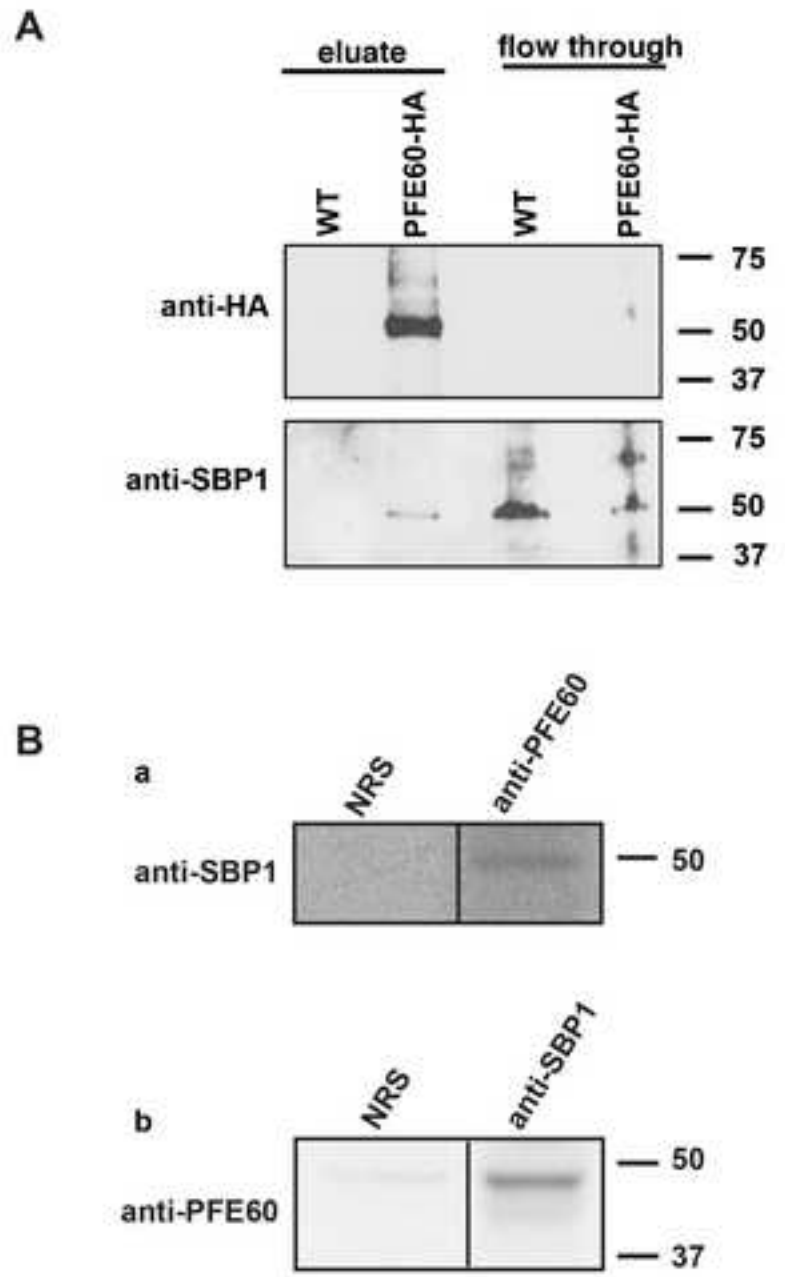

Figure 6

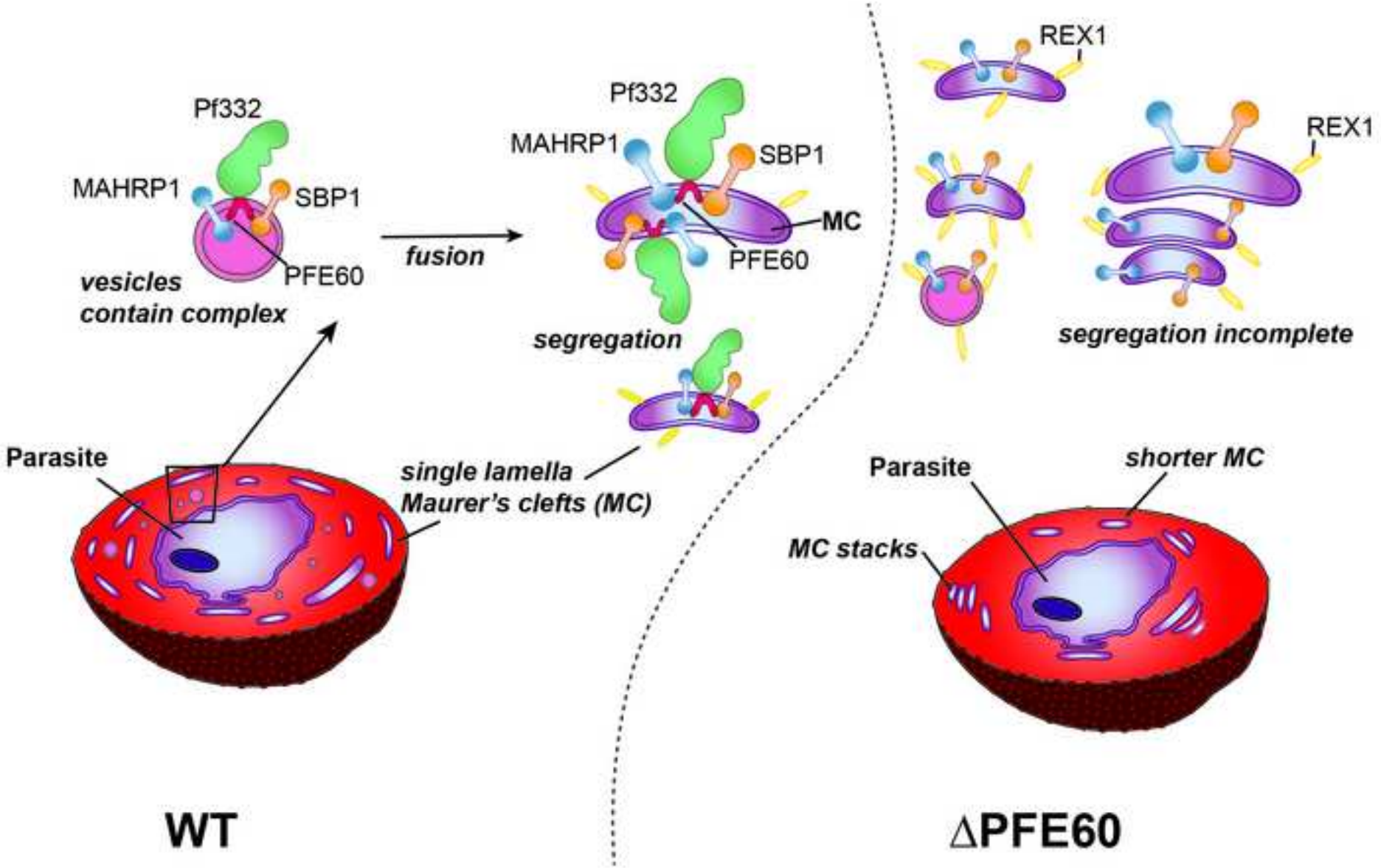

978 **Highlights**

979 • Deletion of *Plasmodium falciparum* export protein 60 (PFE60) leads to shorter and
980 more stacked Maurer's clefts (MC).
981 • Virulence complex protein Pf332 is not efficiently trafficked in the absence of PFE60.
982 • PFE60 does not require its transmembrane domains for trafficking to MC.

983
984